Polysaccharide root exudates and rhizosheaths in barley

Cameron Colclough

Submitted in accordance with the requirements for the degree of
Master of Science by Research

The University of Leeds
School of Biology

September 2021

The candidate confirms that the work submitted is their own and that appropriate credit has been given where reference has been made to the work of others.

In Chapter 3, work on rhizosheath screens included in Table .4 was undertaken by members of the James Hutton Institute, Dundee, UK. Data was analysed and summarised by the candidate.

Acknowledgements

A special thanks to Dr. Tim George and Lawrie Brown at the James Hutton Institute for their initial work on the barely genotypes, providing the seed stock, rhizosheath and root hair data, and advice on the barley cultivars.

My time in the Knox group has been one of pleasure. The generosity of time and guidance that has been shown has both moved and motivated me. I have learnt so many invaluable skills, both technical and personal, that I will carry forward throughout life. But no greater lesson has been learnt than this; that it is not the knowledge and wisdom one has to offer to others, but in the patience and kindness with which they are imparted, that their true benefit is revealed. In this regard, I would like to thank Jumana Akhtar, Professor Paul Knox and Sue Marcus, for none have shown such fortitude and humour, in circumstances so bleak, than they.

Abstract

Casings of soil surrounding plant roots, ubiquitous in cereals, are known as rhizosheaths. They have been proposed as facilitators in root-soil relationships and water dynamics in periods of drought. Rhizosheaths are formed by the entanglement of soil particles in root hairs and the action of adhesive molecules exuded by roots, within which high molecular weight (HMW) polysaccharides have been indicated as key factors. But the glycobiology of cereal exudates is only beginning to be understood. This investigation utilised three techniques to obtain root exudates: hydroponics, short seedling incubations in water and soil-suction-lysimeters. Surveying with a panel of monoclonal antibodies directed to cell wall polysaccharides, identified arabinogalactan-protein (AGP), xyloglucan, and heteroxylan epitopes across the different exudate collection methods and a range of barley genotypes. This glycan profiling was used in conjunction with spatial analysis of polysaccharide exudates; seedling prints on nitrocellulose sheets characterised the patterns of polysaccharide release from along the root axes including a xylogalacturonan epitope (LM8) previously only associated with root apices. Immunofluorescence microscopy established that certain AGP epitopes and a novel beta-glucan epitope are abundant at root hair surfaces of barley plants. From these results it is proposed that groups of glycan epitopes have distinct functions; those presented on root hairs are associated with soil binding and other epitopes provide services for a developing root system. Further analysis into root exudate-soil interactions suggests the adhesive capacity of the HMW components of exudate, in a soil-binding assay, is linked to the rhizosheath weight of barley roots. But also that is likely there is a trade-off in carbon allocation by the plant between root growth and HMW exudation. Such work can hopefully build into the body of knowledge of root systems that can one day influence targeted crop breeding strategies to mitigate against drought.

Table of Contents

List of Tables

List of Figures

List of Abbreviations

AGP	Arabinogalactan-protein
ANOVA	Analysis of Variance
brb	Bald Root Barley
CI	95% Confidence Interval
cvs	Cultivars
ELISA	Enzyme-linked Immunosorbent Assay
FAO	Food and Agriculture Organisation
FITC	Fluorescein Isothiocyanate
GLR	Glutamate Like Receptor
GSP	Grain Softness Protein
HMW	High Molecular Weight
HRP	Horseradish Peroxidase
HSD	Tukey's Honestly Significant Difference Test
JIM	John Innes Monoclonal
KDa	Kilo Dalton
LM	Leeds Monoclonal
LMW	Low Molecular Weight
MAbs	Monoclonal Antibodies
OsCDPK	*Oryza sativa* Calcium Protein Dependent Kinase
OsRHL	*Oryza sativa* Root Hairless Six Like
PBS	Phosphate Buffered Saline
QTL	Quantitative Trait Loci
SD	Standard Deviation

Chapter 1
Introduction

1.1 Introduction

Over 35% of the world's terrestrial area is under agriculture, a third of which is devoted to arable crops, which provide 55% of the world's calorie intake (Cassidy *et al*. 2013; FAO UN, 2018). The farming of arable crops relies heavily on access to water and nutrients within the soil and without adequate supplies of either, yield reductions and total crop failure can result (Samarah, 2005; Masood *et al.*, 2011). Water and nutrient shortages often result in the greater irrigation and tillage of cropland (Tilman *et al.*, 2002), but this too can be detrimental as these processes increase the susceptibility of agricultural soils to degradation through erosion (Montgomery, 2007). Soil degradation has a significant negative impact, altering many critical ecological services and causing the transformation of land from productive to marginal (Schulte *et al.*, 2014; Van Oost *et al.*, 2007; Pimentel and Burgess, 2013). These issues become ever more pressing as instances of drought are exacerbated by global warming, leaving crops increasingly vulnerable to water shortages (Praba *et al.*, 2009; Cook *et al*., 2018). A plant's root system is the main site of uptake for water and nutrients and, through phenotypic plasticity, allows a plant to cope with changes in the availability of these resources in the soil (Hodge, 2004; Ehdaie *et al.*, 2012). Manipulation of specific root traits that can maximise the performance and yield of crops under resource-deficient conditions, therefore, provides a useful tool in maximising the food production output of cropland (Brown *et al.*, 2017; Lynch, 2019).

1.2 The rhizosphere and the rhizosheath

The rhizosphere is the total volume of soil that is influenced by the root, this includes soil affected by various root-microorganism associations, such as the extension of fungal hyphae (Mathesius *et al.*, 2015), as well as how the root system alters the soil's abiotic factors through nutrient and water depletion (York *et al.*, 2016). The rhizosheath is a clearly distinguishable subsection of the rhizosphere, it is formed from the soil directly surrounding the root, and is defined as the mass of soil adhering to the root upon uprooting (George *et al.*, 2014). Confusion between various different root-soil terminology requires codification of each to enable

comparison and reproducibility between experiments. The definitions, as they will be used here, are listed in Table. 1 and visualised in Figure. 1. One of the most common confusions and a problem identified by both York *et al*., (2016) and Pang *et al*., (2017) is the interchangeable, but incorrect, use of the terms rhizosheath and rhizosphere, specifically the mislabelling of rhizosheath soil as rhizosphere soil. This is presumably due to the more conceptual nature of the rhizosphere compared to the rhizosheath, thus making it more difficult to quantify. In contrast the rhizosheath is a more obviously identifiable trait in a plant and differences can be observed with the naked eye (Smith *et al*., 2011; Delhaize *et al,* 2012; Brown *et al.,* 2017). Adoption of a generalised method for rhizosheath collection and measurement is needed to reduce this instance of misidentification, this would also enhance the literature, allowing for better comparisons between studies (Pang *et al*., 2017). Here it is suggested that the methodology designed by Brown *et al*., (2017) is used because of its ease of operation and its applicability across different clades of plants.

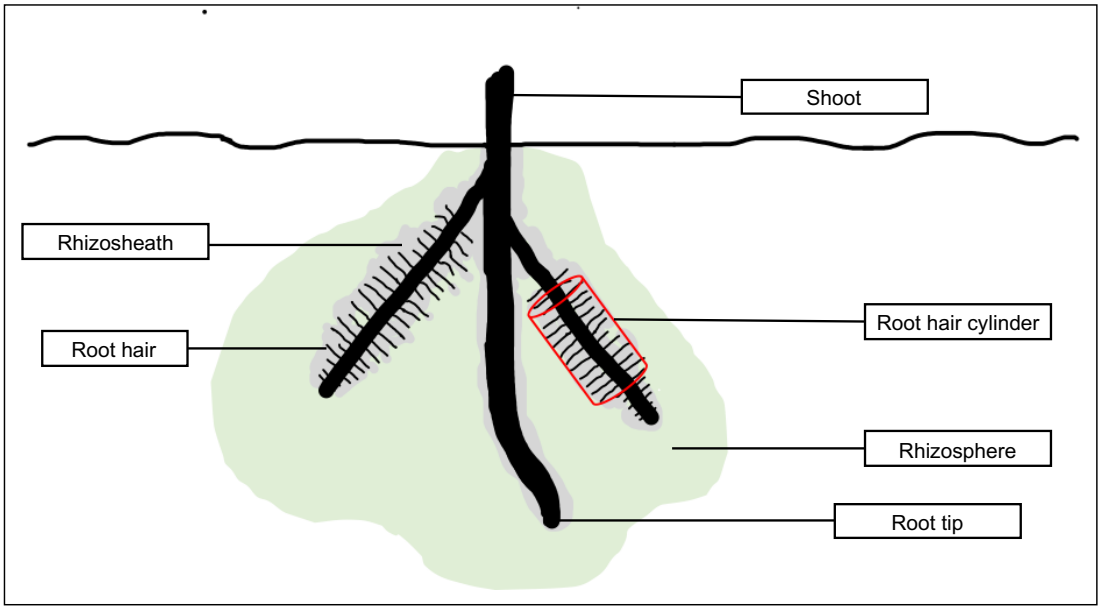

Figure.1 The key features of root system involved in rhizosheath formation and exudate release (Modified from Pang *et al.,* 2017) including the different natures of the rhizosheath and rhizosphere, the root tip from which root cap cells are shed along with polysaccharides and lipids, forming mucilage (Koroney *et al*., 2016) and how the root hair cylinder is measured, as a consequence of root hair length (Yang *et al*., 2017).

1.2.1 Rhizosheaths and abiotic stress tolerance

Rhizosheaths were first observed in arid climate plants (Volkens, 1887), and are ubiquitous in plants grown in dry, sandy environments (Hartnett *et al.*, 2013). This, along with rhizosheaths being larger and adhering to the root more strongly in dry soils compared to moist ones (Watt *et al.,* 1994), has meant the rhizosheath has been linked with adaptation to cope with drought. However, the mechanisms behind how rhizosheaths function in drought tolerance are still not fully understood. One-way rhizosheaths provide protection against drought is by enabling water to be continually drawn towards the root from surrounding soil even in low moisture conditions. As roots dry out they shrink, this causes air gaps to form between the root and surrounding soil (North and Nobel, 1997). These air gaps reduce the hydraulic conductivity (the ability of water to move through pores) of the soil, rhizosheaths help to minimise these air gaps by keeping roots moist and in constant contact with adjacent soil (North and Nobel, 1997; Carminati *et al.*, 2017). The movement of water to roots in dry soils is also influenced by the polysaccharide-rich secretions of roots, which form a gel like matrix called mucilage (Table.1). Whilst mucilage is most often associated at the root tip, some does move into the soil surrounding the root (Vermeer & McCully, 1982). Mucilage absorbs and retains moisture well, this keeps hydraulic conductivity of the soil close to the root high, enabling water to flow to the root even in dry conditions (Read & Gregory, 1997; Ahmed *et al.*, 2014). It has also been proposed that rhizosheaths aid in the retention of water close to the root, stopping it completely drying out, as dried secreted mucilage prevents waterflow out from the rhizosheath, allowing the rhizosheath soil to retain a greater water content than the surrounding soil (Young, 1995; Ahmed *et al.*, 2016). These two, seemingly contradictory, functions of exudate released into rhizosheath soil; that it can both facilitate the movement of water to the root but also retain it around the root, could arise from day-night cycles of fresh exudate release and drying out from transpiration (McCully 1995). So, when it is newly formed polysaccharide-rich exudate enables water acquisition, but after successive wetting and drying it acts to prevent older roots sections from desiccation (Ahmed *et al.*, 2016).

It has been reasoned that the rhizosheath formation by the plant evolved to improve a root system's drought tolerance, but that because of its multi-trait nature, it also provides a variety of other complementary functions for the plant, such as nutrient acquisition (Smith *et al*., 2011; Brown *et al.*, 2012; Haling *et al.*, 2013). An increased

ability for water uptake in dry soils by the rhizosheath would also facilitate access to water soluble nutrients such as nitrates, as these move by mass flow to the plant (Barber *et al*., 1963; North and Nobel, 1997). Rhizosheaths also help plants obtain nitrogen, by mediating interactions with beneficial microorganisms. Root exudates provide a carbon source which enables the colonisation of rhizosheath soil by diazotrophs which in turn provide plants with a source of fixed nitrogen (Othman *et al.*, 2004; Bergmann *et al.*, 2009). For water-insoluble nutrients such as phosphorus, which move to the plant by diffusion (Barber *et al*., 1963), maximising the volume of soil explored is key to suitable uptake. Root hairs are advantageous for phosphorus acquisition as they increase a root's surface area (Bates & Lynch, 2001; Gahoonia & Nielsen, 2004), they are also a key determinant in rhizosheath size (Delhaize *et al.*, 2012; Haling *et al.*, 2014). Barley (*Hordeum vulgare* L.) plants with longer root hairs and larger rhizosheaths had greater shoot phosphorus accumulation and crop yield compared to lines with short root hairs and smaller rhizosheaths (Brown *et al.*, 2012). Being the intermediary zone between the plant root and surrounding soil, and strongly linked to root hair length, rhizosheaths could play a significant role in non-water soluble nutrient uptake (Brown *et al.*, 2012) although its effect in this area is still not wholly understood.

1.3 Rhizosheath formation

The rhizosheath is formed by two main processes; (1) the action of root hairs entrapping soil particles around the root (Moreno-Espindola *et al.*, 2007; Brown *et al.*, 2017) and (2) the bio-adhesive properties of exudates (Vermeer and McCully, 1982; Watt *et al*., 1994; Galloway *et al.*, 2020). Root hairs are the protruding extensions from specific root-hair-cells, they vastly increase a plant's root surface area allowing for greater nutrient and water uptake (Libault *et al.*, 2010; Haling *et al.*, 2013; Grierson *et al.*, 2014). They extend out from the root in all planes forming a quantifiable cylinder encircling the root termed the root-hair cylinder (Fig. 1) (Yang *et al.*, 2017). Root hairs are a key component in the trapping of soil particles around the root, and their presence is required for rhizosheath formation - root hairless mutants are not able to form a substantial rhizosheath (Brown *et al.*, 2012; Haling *et al.*, 2014; George *et al.*, 2014). However, the effect of root hair length on rhizosheath size varies between species. In wheat (*Triticum aestivum* L.), root hair length strongly influenced rhizosheath size (Delhaize *et al*., 2012), and a greater root hair cylinder volume, a direct consequence of root hair length, also produced larger rhizosheaths in several species within the grass family *Poaceae* (Haling *et*

al., 2010a). On the contrary, this doesn't appear to be the case in barley, where there was no discernible difference in rhizosheath size between lines with short or long root hairs (George *et al.*, 2014). Similarly, in chickpea (*Cicer arietinum* L.) the comparatively larger rhizosheath weight of one cultivar to another was attributed to its greater mucilage production, as there was no significant difference in root hair lengths between the two lines (Rabbi *et al.*, 2018). Recent work suggests that not only do root hairs aid in mechanical trapping of soil but that they also are a major secretion site of polysaccharides that increase soil's adhesion to the root. The barley root hairless mutant *brb* (Gahoonia *et al.*, 2001) exhibited much lower glycan epitope signals for a variety of polysaccharides with known adhesive properties compared to its wild type counterpart (cv. Pallas); with the rhizosheath of *brb* almost four times times smaller in mass than that of Pallas (Burak *et al*., 2021). Root hairs evidently perform an important function in forming the rhizosheath across species, however the contrasting results regarding the effectiveness of root hair length on rhizosheath weight, highlights the interaction of numerous factors in rhizosheath maintenance (Brown *et al.*, 2017).

Table.1 The definitions of root- related terminology (modified from Pang *et al* ., 2017)

Term	Definiton	Reference
Rhizosheath	The mass of soil adhering to the root upon uprooting	George *et al* ., 2014
Rhizosphere	The total volume of soil influenced by a root system and bacterial and fungal associations, inc. through nutrient depletion	Mathiues *et al.* , 2015
Root hair cylinder volume	Volume contents of the cylinder encircling the root created by root hairs (Fig. 1)	Yang *et al* ., 2017
Exudate	The range of organic and inorganic compounds released by a plant root, bacteria or fungi	Walker *et al.,* 2003
Mucilage	Exudate assocaited with the root tip (Fig. 1) consisting of matrix of shed root cap cells and polysaccharide and lipid factors	Koroney *et al* ., 2016; Durand *et al* ., 2009; Read *et al* ., 2003;

A range of high-molecular weight (HMW) and low-molecular weight (LMW) compounds have been identified as being released by organisms into surrounding soil, including those from plant roots but also fungal and bacterial secretions (Walker *et al.*, 2003; Oburger & Jones, 2018). These molecules, termed exudate, have long been theorised as key components in a root system's drought tolerance, nutrient acquisition, and defence and communication (Driouich *et al.* 2013; McCully, 1999; Read *et al.* 2003). Those compounds found to be released by barley roots are listed in Table. 2. Root mucilage is a specific form of plant root exudate, deposited from the root tip (Fig.1), it consists of a matrix of shed root cap cells and

associated polysaccharide and lipid factors (Read *et al.*, 2003; Durand *et al.*, 2009; Koroney *et al.*, 2016). Polysaccharides exudates however, are not just released at root apices, they have been detected from along the length of the root axes (Galloway *et al.*, 2020). The release of root exudates into the soil is clearly an important process for plants, as between 2% and 20% of all carbon assimilated by a plant is estimated to be released into the soil; exact figures however, are hard to quantify due to the methodological challenges of *in situ* soil experiments (Kuzyakov & Domanski, 2000; Walker *et al.*, 2003). What is known is that the amount of carbon released is influenced by numerous factors including; plant species, the microbial composition in the soil and the plant growth stage - younger plants releasing more carbon from roots than older ones (Kuzyakov & Domanski, 2000; Cheng & Gershenson, 2007). The mechanisms of exudate release are not wholly understood, but it is clear that they vary based on the molecular weight of the compound. Low-molecular- weight cell metabolites can diffuse across root cells into the soil, down concentration gradients, with some also moving through channels within plasma membranes (Oburger & Jones, 2018). Other LMW components such as iron-acquiring *phytosiderophores,* are actively released by roots (Oburger *et al.*, 2014). In contrast relatively little is known about the mechanisms of release of HMW compounds, but is thought to be derived, at least in part, from lysed-cell contents and through exocytosis of vesicles formed in the Golgi apparatus (Bacic *et al.*, 1986; Jones and Morre 1973).

Table. 2 Compounds identifed in Barley root exduates

	Compound	Reference
Low-Molecular-Weight		
Amino acid	Asparagine, Aspartic acid, Serine, Glycine, Glutamie acid, Threonine, α-Alanine, Proline, Tyrosine, Valnine, Phenylalanine, Isoleueine, Leueine	Naveed *et al* ., 2017; Vančura, 1964
Organic acid	Oxalic acid, Malic acid, Glycolic acid, Succinic acid, Fumaric acid, Butanoic acid, Aetoacetic acid	Naveed *et al* ., 2017; Vančura, 1964
Sugar	Maltose, Galactose, Glucose, Arabinose, Xylose, Ribose, Rhamanose, Deoxyribose, Glulose	Naveed *et al* ., 2017; Vančura, 1964
Sugar acid	Ribonioc acid, Gluconic acid, Threonic acid	Naveed *et al* ., 2017
High-Molecular-Weight		
Glycan residues	α-1-5-L-arabinan, extensin, arabinogalactan-protein (AGP), heteroxylan, xylogulcan	Galloway *et al* ., 2021

1.3.1 Overcoming the challenges to the study of polysaccharides released by plant roots.

Plant polysaccharides are diverse and structurally complex polymers which encompass a vast assortment of different oligosaccharide residues (Lee *et al.*, 2011). They are the building blocks of plant cell walls and also form a key HMW fraction of exudates (Galloway *et al.*, 2020). Polysaccharide factors have a history of recognition as bio-adhesives, with work focusing on their capacity to aggregate soil particles (Tisdall and Oades, 1982; Cheshire and Hayes, 1990). This implicates them in soil binding processes, such as rhizosheath formation (Galloway *et al.*, 2020). But due to the technical difficulties of collection, analysis has often been restricted to mucilage secreted at root tips (Oburger & Jones, 2018). Rhizosheaths, however are maintained along the length of the root (Brown *et al.*, 2017) and so this restriction has limited the understanding of polysaccharide exudates in rhizosheath formation. Previous analysis of the polysaccharide components of exudates has relied on chemical analysis of monosaccharide- linkages (Bacic *et al*., 1986; Moody *et al.* , 1988). Whilst this is useful, it does not provide the order or structure of sugar molecules within polysaccharides, and so only gives indications as to the molecules present (Carpita & Gibeaut, 1993). Identification of specific exudate molecules or associated complexes which function in soil binding and rhizosheath formation is lacking, both in characterising their structure and the physiological processes behind their release.

Monoclonal antibodies (MAbs) are specific and sensitive molecular tools which allow for the tracking of polysaccharide across various circumstances (Lee *et al.*, 2011). They are exceptional molecular discriminators, that recognise specific regions (epitopes); sequences of sugar residues contained on larger polymers (antigens) (Pattathil *et al.*, 2012). Monoclonal antibodies allow for the identification of polysaccharides *in situ*, as well as providing quantitative measures of the amounts in mixtures (Hervé *et al*., 2010). Monoclonal antibodies enable the carbohydrate contents of root exudates to be analysed against worldwide collection of almost 200 probes (Pattathil *et al.*, 2012). As well as tracking their release from tissues (Hervé *et al*., 2010). It was this use of MAbs that first identified polysaccharide secretion from along the root axes and not just from the root tip (Galloway *et al.*, 2020). The versatility of MAbs also allows for the visualisation (under immunofluorescence microscopy) of where polysaccharides are at root

surfaces which may provide insights into their function. The detection of the xylan LM11 epitope coating root hairs and soil surrounding the root, confirmed its significance in rhizosheath construction (Galloway *et al.*, 2020).

In maize, root tip mucilage is rich in cell wall related pectic polysaccharides, particularly homogalacturonan and xylogalacturonan (Willats *et al.*, 2004; Cannesan *et al.*, 2012; Koroney *et al.*, 2016). Xylogalacturonan has been associated with plant cell defence against microbes, due to its relative inability to be digested by enzymes often secreted by pathogens (Jensen *et al.*, 2008; Driouich *et al.*, 2013). Comparatively, exudate collected from maize hydroponics contained only low levels of homogalacturonan and no signals for other pectic polysaccharides (Bacic *et al.*, 1986; Galloway *et al.*, 2020). This low presence of pectic polysaccharides epitopes in the surveyed HMW fraction of exudate could reflect their relative water insolubility (Guo *et al.*, 2017; Naveed *et al.*, 2017; Galloway *et al.*, 2020). It could also suggest that carbohydrate exudates released at different areas of the root have different functions. Those secreted at root caps aid in lubrication as the root tip descends in soil and in plant-pathogen defence (Iijima *et al.*, 2004; Driouich *et al.*, 2013) and those from along the root function in soil binding and rhizosheath formation (Akhtar *et al.*, 2018; Galloway *et al.*, 2020). Numerous polysaccharides were found to be released from along cereals root axes by the use of MAbs, these included xyloglucan, multiple xylan epitopes and signals for arabinogalactan-proteins (Galloway *et al.*, 2018, 2020). Xyloglucan is released from an assortment of species, including basal land plants, it has also been displayed as an effective binder of both small and large soil particles (Akhtar *et al.*, 2018; Galloway *et al.*, 2020). An interesting feature is that xyloglucan has comparatively low prevalence in grass cell walls (O'Neill & York, 2018), indicating that some polysaccharides could be specifically released because of their soil aggregating capacities as opposed to being a beneficial consequence of dead and broken down-cell shedding. This, in conjunction with evidence for the presence of carbohydrate-macromolecules, containing a variety of different glycan epitopes within root exudate (Galloway *et al.*, 2020), demonstrates the structural complexity of polysaccharides secreted by roots and also their highly derived functions. Even though the full structures of these exudates are not fully understood, the value of identifying their constituent role in rhizosheath formation is clear.

1.3.2 Genetic factors that underlie rhizosheath production

The multitude of factors that influence the rhizosheath suggest that it is controlled by multiple genes at different loci. Work has begun to identify and assess the genetic mechanisms that constitute the basis of rhizosheath formation and maintenance. In wheat, rhizosheath weight is highly heritable (Delhaize *et al*., 2015; James *et al.*, 2016) and initial screens of cereal populations have realised several quantitative trait loci (QTL) of interest. Two of the QTL identified by Delhaize *et al*., (2015) were proposed to underpin a wheat homologue of the rice gene *OsRHL1*- a basic helix-loop-helix transcription factor which is known to influence root hair development (Ding *et al.*, 2009). Screening of a spring barley population revealed several QTL all on the same chromosome, all affecting overall weight of the rhizosheath, and from this several candidate genes were identified (George *et al.*, 2014). The equivalent genes in other plants are involved in calcium signalling. One of the candidate genes identified by George *et al*. (2014) is barley homologue of the rice gene *OsCDPK7*, which expresses a calcium-dependent protein kinase, important in drought and salt stress tolerance (Saijo *et al.*, 2000). The second is again a barley homologue of a rice gene; *GLR3.1* a glutamate-like receptor involved in cell proliferation and the development of plant roots (Li *et al.*, 2006). *Arabidopsis GLR3.1* encodes proteins needed for calcium ion channel maintenance (Kong *et al.*, 2016). Calcium's role as an intracellular second messenger in plant root and root hair growth has been widely acknowledged (Hepler *et al*., 2001; Foreman *et al.*, 2003; Hetherington and Brownlee, 2004). Interference with GLR3.1, in rice seedlings, showed an increase root cap cell shedding at the root tip (Li *et al.*, 2006) which is a key secretion site of polysaccharide containing mucilage (Koroney *et al.* 2016; McCully, 1999). The QTLs identified in barley linked to glutamate-like receptors may also underlie the production of root-cap associated mucilage. Further work to elucidate the genes and downstream processes involved is essential.

1.4 Rhizosheaths as a target for crop breeding in barley

With over 50 million hectares farmed, and 178 million tonnes of grain produced, barley (*Hordeum vulgare* L.) is one of the world's most cultivated cereal crops (FAO UN, 2018). Whilst much of barley production is used as livestock feed and in beverage production, it still provides an invaluable food source for many peoples (Newman & Newman, 2006). The ecological range of barley is far larger than most other cereal crops (Newton *et al.*, 2011). Together with its ability to grow at high

altitudes, and its comparative hardiness against salt and drought stresses, mean it has been identified as a candidate for the agricultural exploitation of marginal lands (Colmer *et al*., 2006; Kosová *et al*. 2014; Moza and Gujral, 2016; Lister *et al*., 2018). Barley is also an important model system for cereals and ecological adaptation, because of the successful mapping of it genome, and the range of genetic and biotechnological tools available for use with it (Mayer *et al.*, 2012; Harwood, 2019). Improving upon barley's already favourable attributes through root traits, like rhizosheath size, could provide relief from a collection of agronomic problems. Globally, water is a major limiting resource to plant growth (Cook, *et al*., 2018) and the rhizosheath provides a root system with ability to tolerate drought stress. This along with rhizosheaths being found in plants across the angiosperm phylogeny (Duell and Peacock, 1985; Smith *et al*., 2011; Brown *et al.*, 2017), make it a potential avenue for manipulation, through targeted breeding, across a range of staple crops (Brown *et al.*, 2017). Research into how rhizosheaths form and their functions is an important area in regard to improving global food cropping systems.

1.5 Aims and Objectives

Whilst the evidence for rhizosheath formation is strong, the knowledge of how the mechanisms behind rhizosheath formation operate, is patchy especially in regard to the role of exudates. In order to address this knowledge gap, this investigation is designed to test the primary question of whether larger rhizosheath genotypes will exhibit a greater release of soil binding polysaccharides than the small rhizosheath genotypes. I aim to focus on the following key objectives**.**

(1) To analyse the polysaccharide profiles secreted by different barley genotypes across a range of collection systems.
(2) To track and characterise the regions of release of polysaccharide epitopes from barley plants
and how this may relate to their function
(3) To assess how the polysaccharide profiles may pertain to differences in the rhizosheath between barley genotypes

Chapter 2
Materials and methods

2.1 Plant materials and growth conditions

Barley (*Hordeum vulgare* L. cultivars Aluminium, Beatrix, Eunova and Starlight; provided by the James Hutton Institute, Dundee UK) representing a panel of elite spring barley genotypes planted in the UK from the past 20 years (George *et al.*, 2014) were selected for use. The lines selected represent two genotypes deemed to have a large rhizosheath (Eunova and Starlight) and two a small rhizosheath (Aluminium and Beatrix) from a screen at the James Hutton Institute. The barley seeds were germinated in 100 mm x 100 mm Petri-plates (Sarstedt, Australia) on 1% agar (A792; Sigma-Aldrich USA) media in a standing growth cabinet (MLR-325-PE; Sanyo, Japan) at 22°C and a 16-h photoperiod with an average light level of 634 µmol m^{-1} s^{-1}. All seeds were germinated under these conditions prior to use.

2.2 Hydroponics system

Barley seedlings were grown on agar plates (outlined in Section 2.1). The seedlings were then moved into a hydroponics system at seven days old. Six seedlings were removed from the agar, making sure none remained attached to the roots. The seedlings were then placed in sponge supports in holes within a polystyrene foam board, with the roots descending below the board and the plant stems sticking out above (Fig. 2). This was then placed over a nine-litre bucket containing nine litres of half-strength Hoagland's nutrient solution (7.2 g/ 9 L; H2395, Sigma-Aldrich USA). The solution was continuously aerated (11.2 L /min) with an aquatic pump (All Pond Solutions, UK) and the seedlings left to grow for 14 days in glasshouses at 22°C with a 16-h photoperiod and an average light level of 1382 µmol m^{-1} s^{-1}. During the growth period buckets were topped up with de-ionised water to maintain a volume of nine litres of growth media. After two weeks the plants were removed from the system and weighed and measured, recording both their total root wet biomass, as well as the length of the longest root of each plant. The roots were dried in an oven (Genlab incubator, Genlab, UK) at 65 °C until they reached a constant mass to obtain the dry biomass.

2.3 Collection of high-molecular weight root exudate from hydroponics

Once the plants were removed the hydroponics growth media (hydroponate), it was then filtered to obtain the high-molecular weight (HMW) fraction, initially through filter paper (Whatman Grade 2 V, 240 mm; GE Healthcare, Germany) to remove root debris and root hairs. The hydroponate was then put through a Centramate ultrafiltration system (FScentr005K10; PALL Life Sciences, USA) with a 30 KDa cassette at 500 mL/min leaving the HMW fraction of the hydroponate (> 30 KDa), this reduced the nine litres to around 120 mL and was then split over four 50 mL centrifuge tubes (Corning, USA). The HMW fraction of root exudate was then frozen overnight at -80°C and lyophilised (Heto LyoPro 6000, USA) for four days. The dry material was then rehydrated to around 15 mL and dialysed using a 3.5 KDa cut-off membrane (Spectra/pro, Spectrumlabs, USA), in order to remove salts from the liquid, against five litres of de-ionised water at room temperature for four days changing the water twice a day. The HMW exudate was then frozen again overnight at -80°C and lyophilised again for four days and the dry HMW material weighed and recorded.

2.4 Collection of root exudate from seedlings

After 10 days growing on agar plates (method outlined in Section 2.1) the barley plants were removed from the plate and their root systems placed in 7 mL bottles (Sarstedt, Australia) containing 5.5 mL of de-ionised water, and left to exude for 4 h, making sure to keep only their roots submerged and not their seed or shoot (Fig. 2). The seedlings were then removed, weighed, and their longest root measured.

2.5 Collection of root exudate from plants grown in soil

Barley seedlings were grown on agar plates (as in Section 2.1) for 10 days. Six seedlings were then placed in a 160 mm diameter x 140 mm height pot containing a 50:50 (volume per volume) mix of sand (horticultural silver sand, RHS, UK) and 2 mm sieved topsoil (Norfolk topsoil, Baileys of Norfolk, UK) by making a hole in the pot about 40 mm deep and placing the root system in and covering with the soil mixture. The seedlings were arranged in a circular pattern around the pot with space in the middle. The plants were then left to grow in glasshouses at 22°C and a 16-h photoperiod with an average light level of 1382 µmol m^{-1} s^{-1} and watered every two days allowing the plant to settle into their new environment. After five days a soil-suction lysimeter (HI-83900-30; Hanna instruments, USA) was pushed down

into the sand-soil in the centre of the pot to about a depth of 50 mm, until the ceramic base of the lysimeter was covered. The plants were left to grow for a further five days. The pot was then watered with 200 mL of wa ter and a 30-kilopascal vacuum pulled on the lysimeter by the syringe, the clip was then attached to stop any air flowing back in and the lysimeter was left to draw in water-containing exudate for one hour. After this the clip was released and the water was pulled through the lysimeter into the syringe where between 10 mL and 15 mL of exudate was collected and transferred to a 15 mL centrifuge tube (Corning, USA).

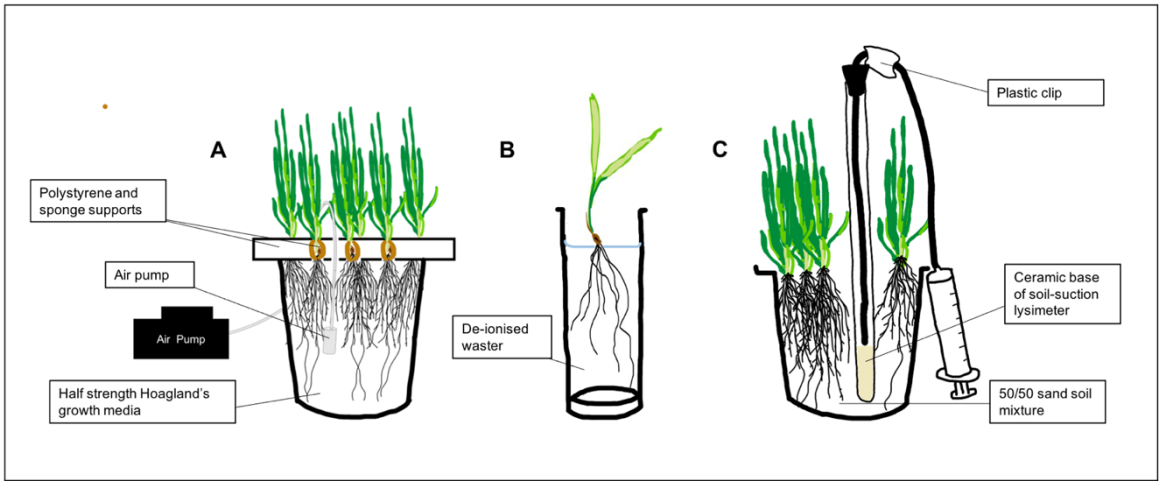

Figure. 2 Collection methods of root exudate from barley plants.

Barley cultivars (*Hordeum vulgare* L., cvs Aluminium, Beatrix, Eunova and Starlight) were germinated on agar plates. (A) Collection of high-molecular-weight (HMW) fraction of root exudate by hydroponics, six seedlings seven-day old seedlings were placed in sponge supports in holes within a polystyrene foam board which was placed over a 9 L bucket half-strength Hoagland's nutrient solution. The solution as continuously aerated by a pump and the seedlings left to grow for 14 days at in glasshouses. The media was then filtered to remove low-molecular-weight components of the exudate (< 30 KDa), lyophilised, dialysed against de-ionised water, and lyophilised again to attain a dry mass of HMW root exudate. (B) Ten-day old barley seedlings were removed from agar plates and their root systems placed in 7 mL bottles containing 5.5 mL of de-ionised water and left to exude for 4 h. (C) Six seedlings were grown in a pot containing a 50/50 mix of sand and sieved topsoil in glasshouses. A soil-suction lysimeter was pushed down into in the centre of the pot until the ceramic base of the lysimeter was covered. The pot was then watered, and a vacuum pulled on the lysimeter by the syringe the clip was then locked. After an hour the clip was released and the water was pulled through the lysimeter into the syringe. The different collection methods offer different comparisons of root exudate (A) a per unit weight comparison (B) per unit volume and (C) to explore exudate release in soil as a comparison to that in water.

2.6 Enzyme-Linked-Immunosorbent-Assay (ELISA)

Samples of the collected exudate from either, hydroponics, seedlings or the soil lysimeter were diluted into phosphate-buffered saline (PBS) (Severn Biotech, UK). The samples were then titrated down a 96 well microtitre plate (Thermo Fisher Scientific, Denmark) with the last row left as a negative control containing no-antigen. The plates were then placed in the fridge at 4°C overnight. The plates were then rinsed by submerging three times in tap water and then patted dry. The addition of 200 µL of 5% weight per volume of milk powder (Marvel, UK) dissolved in PBS (milk-PBS) to each well was followed by incubation at room temperature for an hour. The plates were then rinsed as, before in tap water 15 times and dried. The plates were then incubated with rat primary antibody, a 1 in 10 dilution of hybridoma supernatant (Table. 3) in milk-PBS, 100 µL per well, for a further hour. Again, the plates were then rinsed as before, 15 times and dried and then incubated with 1 in 1000 dilution of the secondary antibody anti-rat HRP (Immunoglobulin G coupled with horseradish peroxidase; A9552 Sigma-Aldrich USA) in milk-PBS, 100 µL per well, for an hour. After washing again another 15 times and drying the plates, 100 µL per well of the substrate (9 mL de-ionised water, 1 mL 1 M sodium acetate buffer, 100 µL of 3,3’,5,5’-tetramethylbenzidine 10 mg/mL in dimethyl sulphoixde (T-2885; Sigma-Aldrich, USA) and 10 µL of hydrogen peroxide) was added and left to react for 5 min. After the time had elapsed 50 µL of 2.5 M sulphuric acid was added to each well, halting the reaction. The absorbance values for each well were then read using a Multiskan plate reader the SkanIt software (both Thermo Scientific, USA) at 450 nm.

Table. 3 Polysaccharide structures contained within barley root exudate and associated anti-glycan monoclonal antibody

Antigen	Antibody	Reference
Heteroxylan	LM11	McCartney *et al*., 2005
	LM27	Cornuault *et al*., 2015
Xylogucan	LM25	Pedersen *et al*., 2012
Heteromannan	LM22	Marcus *et al*., 2010
Galactan	LM5	Jones *et al*., 1997
Arabinan	LM6-M	Cornuault *et al*., 2018
Homogalactoronan	LM19	Verhertbruggen *et al*., 2009
	LM20	Verhertbruggen *et al*., 2009
Xylogalactoronan	LM8	Williats *et al*., 1998
Arabinoglactan-protien	LM2	Yates *et al*., 1996
	LM30	Wilkinson *et al*., 2017
	JIM13	Knox *et al*., 1991; Yates et al., 1996
Extensin	LM1	Smallwood *et al*., 1995
Beta-glucan	JIM6	Pedersen *et al*., 2012
	10H2	Unpublished
	7E1:B11	Unpublished

2.7 Nitrocellulose seedling printing

The nitrocellulose printing followed the protocol of Willats *et al*., (1998) and Galloway *et al*., (2018). Barley seedlings were grown on agar plates (outlined in Section 2.1) for seven days. Seedlings were then removed from the agar and placed on 9 cm^2 of nitrocellulose (Amersham Protran 0.45 µm, GE Healthcare, Germany) dampened with de-ionised water in a 100 mm x 100 mm weighing boat, for 1 h. The seedling was then removed, and the nitrocellulose left to dry at room temperature, covered with aluminium foil, overnight. The nitrocellulose sheet was then blocked with 22.5 mL of 5% weight per volume of milk powder (Marvel, UK) dissolved in phosphate-buffered saline (Severn Biotech, UK) (milk-PBS) with 0.0025% volume/volume of sodium azide solution (to remove endogenous peroxidases) and incubated on a see-saw rocker (Stuart, UK) with light rocking at room temperature for an hour. Rat primary antibody, a 1 in 10 dilution of hybridoma supernatant (Table. 3) was then added to each weighing boat and left rocking for another hour. After rinsing lightly in tap water, the sheet was then washed with 25 mL of PBS for 5 min, and this was then repeated a further two times. After washing the sheet was incubated with 25 mL of secondary antibody, 1 in 1000 dilution of antibody anti-rat HRP (Immunoglobin G coupled with horseradish peroxidase; A9552 Sigma-Aldrich, USA) in milk-PBS for another hour. After incubation the rinsing and washing stage was repeated again. The following substrate was then

added; 25 mL of de-ionised water, 5 mL chloronapthol (5 mg/mL in ethanol) and 30 µL of hydrogen peroxide and the print left to develop for 15 min, after which the sheets were rinsed with tap water and left to dry overnight between Whatman paper (Whatman 3 mm CHR paper, 580 mm x 680 mm, GE Healthcare, Germany). The nitrocellulose sheets were then imaged on a scanner (Epson v750 Pro, Epson, Japan).

2.8 Immunofluorescence labelling of plant root surfaces

The immunofluorescence labelling of excised root segments followed the protocol outlined by Willats *et al*. (2001) and Galloway *et al.* (2020) Barley plants were grown according to method in section 2.2 and 2.5. The plants were then removed from the soil and 10 mm sections of the roots taken. The root segments were then left in 4% volume/volume paraformaldehyde in PEM buffer fixative solution overnight. They were removed the following day and rinsed twice in phosphate-buffered saline (PBS; Severn Biotech, UK). The root segments were then placed in 12 well cell culture plates (Nunc, Thermo Scientific, USA) and blocked with 2 mL per well of 5% weight per volume of milk powder (Marvel, UK) dissolved in PBS (milk-PBS) and incubated on a see-saw rocker (Stuart, UK) with light rocking at room temperature for 30 min. After an hour had elapsed the milk-PBS solution was pipetted off and 2 mL of PBS solution was added to each well and rocked for 5 min and then pipetted off. This washing step was repeated a further two times. A subsequent 1 mL of rat primary antibody; a 1 in 5 dilution of hybridoma supernatant (Table. 3) in milk-PBS was added to each well and incubated again with gentle rocking for 90 min. The primary antibody was then removed followed by three more 5 min washes with PBS solution. The secondary antibody was then added, 1 mL per well of anti-rat FITC (Immunoglobulin G coupled with fluorescein isothiocyanate; F1763; Sigma-Aldrich, USA), a 1 in 100 dilution in milk-PBS. The wells were washed a third time with 2 mL of PBS 5 min a time, three times and 1 mL per well of a 1 in 10 dilution in PBS of Calcofluor (18909; Sigma-Aldrich, USA) at 0.25 mg/ml was added. Again the wells were washed three times with PBS as before and then 100 µL of 0.1% Toluidine Blue solution (Sigma-Aldrich, USA) was added, making sure all the root segments were well covered, to counteract any autofluorescence from the root segments which is prevalent in grasses (Xue *et al*., 2013). It was then immediately removed, and root segments were rinsed extensively by repeated pipetting and removal of PBS. The root segments were then stored at 4°C in their wells in c. 2 mL of PBS with a drop of Citifluor in PBS (AGR1322, Agar Scientific,

UK) to stop florescence fading. The root segments were then mounted on microscope cavity slides (Agar Scientific, UK) in a drop of Citifluor in PBS before viewing under a microscope (Olympus Optical GX; BX61: Olympus, USA). Images were taken with a Hamamatsu ORCA publisher camera (Hamamatsu, Japan).

2.9 Soil-adhesion assay of high-molecular weight exudates

The soil-binding assay followed the protocol outlined by Akhtar *et al.*, (2018). The high molecular weight fraction of the exudate collected from hydroponics was dissolved in de-ionised water. Nitrocellulose sheets (Amersham Protran 0.45 µm, GE Healthcare, Germany) were cut into 80 mm x 60 mm rectangles, marked with 1 cm^2 squares, and placed in 100 mm x 100 mm weighing boats. Exudates were spotted onto the sheet in 5 µL drops in the marked 10 mm^2 squares starting at decreasing in concentration going down the sheet, the final spot for each exudate being 5 µL of de-ionised water. The weighing boat was then covered with aluminium foil and left to dry for 2-3 h. The sheet was then briefly dipped in de-ionised water for around two seconds, laid in a new weighing boat and covered with sterile sieved < 500 µm topsoil (Norfolk topsoil, Baileys of Norfolk, UK). The weighing was again covered with aluminium foil and left to dry overnight. The next day the now dry sheet was lifted by the corner and lightly shaken with forceps to remove excess soil. The sheet was then dipped into a de-ionised water for 1 sec and then again, using fresh water between dips and sheets. The sheet was then left to dry overnight. The sheets were imaged using an Epson Perfection V750 Pro scanner (Epson, Japan) and Image J and calibration curve equation from Akhtar *et al.*, (2018) used to calculate the amount of soil adhered to each spot.

2.10 Rhizosheath measurements

Barley seedlings were grown on agar plates (outlined in section 2.1) and then the barley plants were grown according to the method in section 2.5. At 10 days in soil the plants were no longer watered to aid in the formation of a detectable rhizosheath. After two weeks the plants were removed by squeezing the pot's sides to loosen the soil and then upending the pot into the hand. The plant root was teased away from the soil with the fingers and shaken very lightly to remove any remaining bulk soil. The whole plant with the rhizosheath attached was then weighed, the rhizosheath was then removed by washing gently under running tap water. The plant was then patted dry and reweighed, the mass of then rhizosheath

was determined. The length of the longest root was measured and recorded. The roots and shoot wet biomass were recorded individually and then the roots dried in an oven (Genlab incubator, Genlab, UK) at 65°C until they were a constant mass to obtain the dry biomass.

2.11 Statistical analysis

All statistical analysis took place within R studio (R Core Team, 2018). A one-way ANOVA was employed to look for the effect of cultivar on differences in root growth and between rhizosheath measurements between at least two groups. To discriminate the differences between individual cultivars Tukey's honestly significant difference test (HSD) was used.

Chapter 3
Results

3.1 A variety of polysaccharides are released from barley roots grown hydroponically

For the initial assessment of the polysaccharide epitopes released from the roots of barley cultivars a hydroponics system was used to grow the plants and collect their root exudate. This system provides easy and efficient method of root exudate collection and aims to simplify the complex interactions of exudate in soil (Oburger & Jones, 2018). Combined with an Enzyme-linked immunosorbent assay (ELISA), which requires a smaller quantity of material and can detect substructures with far greater accuracy in complex mixtures than for other forms of chemical analysis (Lee *et al*., 2011; Galloway *et al.*, 2020), makes it a good method for surveying the polysaccharides present. This investigation focused on identifying the possible polysaccharide epitopes present in each of the barley cultivars root exudate and comparing their relative abundance for the weight of dry exudate used. The investigation then pivoted to evaluate how the root exudate from the barley cultivars differed in their ability to bind soil using a nitrocellulose based assay (Akhtar *et al.*, 2018).

3.1.2 The high-molecular weight root exudate of barley contains xylan, AGP and beta-glucan epitopes

The high molecular weight (HMW) fraction (containing molecules greater than 30 KDa) of the barley root exudate was processed according to section 2.3. This resulted in dry exudate that could be dissolved and probed with an extensive set of Monoclonal antibodies (MAbs) by ELISA. A panel of 12 antibodies was used to probe the exudate. This group of antibodies covered a broad range of pectic polysaccharide, non-pectic non-cellulosic polysaccharide, arabinogalactan-protein, and glucan epitopes. Probing of the barley cultivars root exudate on a per weight basis then took place (displayed in Fig.3). In the HMW exudate isolated from hydroponics the largest signals across all the cultivars came from the xyloglucan (LM25) epitope. There were also strong signals also for arabinan (LM6-M), as well as AGP and heteroxylan epitopes, a similar range to those found to be strongest in wheat root exudate (Galloway *et al.*, 2020).

Antigen	Antibody	Aluminum Mean	Aluminum SD	Beatrix Mean	Beatrix SD	Eunova Mean	Eunova SD	Starlight Mean	Starlight SD
Heteroxylan	**LM11**	0.315	0.179	0.446	0.325	0.271	0.167	0.801	0.036
	LM27	0.487	0.188	0.485	0.447	0.160	0.142	0.031	0.018
Xylogucan	**LM25**	1.348	0.783	2.034	0.111	1.927	0.163	1.428	0.035
Heteromannan	**LM22**	0.434	0.606	0.014	0.045	0.015	0.011	0.017	0.009
Arabinan	**LM6M**	0.322	0.486	0.627	0.531	0.525	0.909	0.540	0.763
Xylogalactoronan	**LM8**	0.007	0.003	0.039	0.023	0.000	0.000	0.107	0.137
AGP	**LM2**	0.126	0.107	0.180	0.156	0.344	0.298	0.314	0.320
	LM30	0.176	0.299	0.904	0.793	0.377	0.358	0.768	1.074
Extensin	**LM1**	0.290	0.303	0.783	0.683	0.329	0.500	0.247	0.335
Beta-glucan	**JIM6**	0.000	0.015	0.000	0.002	0.001	0.002	0.008	0.001
	10H2	0.148	0.157	0.043	0.040	0.013	0.016	0.043	0.024
	7E1/B11	0.589	0.518	0.153	0.039	0.170	0.082	0.190	0.024

Scale: 2, 1.5, 1, 0.5, 0.1

Figure. 3 Heatmap comparison of the polysaccharide epitopes detected per unit weight of the isolated high-molecular weight (HMW) root exudate of barley cultivars.

Barley cultivars (*Hordeum vulgare* L., cvs. Aluminium, Beatrix, Eunova and Starlight) were grown hydroponically in 9 L buckets, and the HMW fractions of root exudate isolated. For each cultivar three (two for Starlight) exudate samples were collected and analysed by indirect ELISA. Values shown are from wells coated with 10 µg mL^{-1} of HMW exudate. Values are the absorbance at 450 nm. Five to six plants were grown in each bucket and this formed one biological replicate, values are the means of 3 biological replicates (Starlight n= 2). Heatmap scale gradient shown on the right. SD; standard deviation, AGP; Arabinogalactan-protein.

3.1.3 Root growth varied between barley cultivars grown under hydroponics

After two weeks of growth in the hydroponics system (section 2.2) the root systems of each cultivar root system were well developed and characterised by many seminal roots and a dense mass of lateral roots. To assess any differences in the root growth of the barley cultivars under the hydroponics system, the lengths of the longest roots (a proxy for overall root length) of every plant in a nine-litre bucket and the total fresh root biomass per bucket were recorded (Fig.4). Each bucket formed a biological replicate and three biological replicates for each cultivar were produced (two for the cultivar Starlight). In order to compare differences in the effect of cultivar on average length of the longest root a one-way ANOVA was used and found to be significant between at least two cultivars ($F = 5.79$, $P = < 0.01$). With regard to differences between the individual cultivars Tukey's honestly significant difference test (HSD) was employed. The mean length of the longest root of Starlight was 71% longer than that of Eunova (P adj. = 0.001, 95% CI = -30.21, -6.15). The differences between all other cultivars were not significant ($P = > 0.05$). Differences in the average total fresh root biomass per bucket were tested for significance and revealed cultivar did have an effect on total fresh root biomass (One-way ANOVA; $F = 5.73$, $P = < 0.05$). The only significant difference between cultivars was the mean total fresh root biomass of Starlight which was 301% greater than that of Eunova (Tukey's HSD, P adj. $= < 0.05$, 95% CI = -20.59, -1.57). Again, the differences between the other cultivars were not significant ($P = > 0.05$). Overall, this revealed that only the root growth of between, the two large rhizosheath cultivars, Starlight and Eunova was statistically different

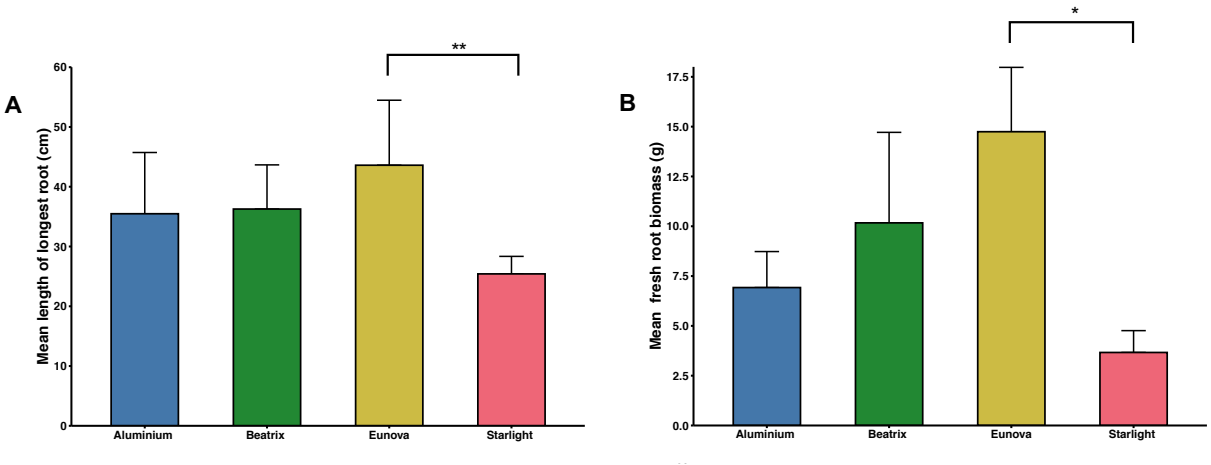

Figure. 4 Mean longest root lengths and fresh weight of seedlings of barley cultivars

Barley cultivars (*Hordeum vulgare* L., cvs. Aluminium, Beatrix, Eunova and Starlight) were grown hydroponically in 9 L buckets. (A) The roots of each plant where then extended the longest root identified and then measured. (B) The total root biomass of all the plants in a bucket was recorded. Five to six plants were grown in each bucket forming one biological replicate. Data points represent the means of three biological replicates (Starlight n= 2). Significance codes; *= $P < 0.05$; **= $P < 0.01$ after means were compared using a one-way-ANOVA and Tukey's Honestly significant different posthoc testing was applied. Error bars show standard deviation.

3.1.4 There was no significant difference in the amount of high-molecular weight root exudate produced by barley cultivars

To try and assess whether a cultivar produced more exudate than another, a gram for gram comparison was conducted (Fig. 5) The mass of collected dry HMW root exudate for each 9 L bucket (one biological replicate) was determined per gram of fresh root biomass from the same bucket. An average value of the biological replicates for each cultivar was then calculated (Beatrix and Eunova n = 3, Aluminium and Starlight n = 2). The effect of cultivar on differences in the average dry mass of HMW root exudate per gram of fresh root biomass were tested and determined not to be significant (One-way ANOVA; F = 1.22 , P = > 0.05).

3.1.5 The high-molecular weight root exudate of barley cultivars had different soil-binding capacities

Whilst the use of MAbs and ELISA sought to identify the polysaccharide contents of root exudate the use of the nitrocellulose-based assay was used to test the exudate's adhesive capacities, in terms of ability to bind soil (Fig.6). The calibration curve equation, from Akhtar *et al.*, (2018), (0.0138*mean-grey-value – 0.0248) was used to convert mean grey values calculated from image J to milligrams of soil bound for each dot of root exudate. The dry HMW root exudate for each replicate of each cultivar was diluted down the nitrocellulose sheet to look at the effect of concentration on the soil-binding capacity. For all the cultivars 50 µg of root exudate bound the most soil. The mean amount of soil bound was significantly affected by cultivar from which the root exudate came between at least two groups (One-way ANOVA; F = 6.67, P = < 0.05). Tukey's HSD post hoc testing showed that between the cultivars Eunova and Starlight (both predefined as large rhizosheath genotypes, see Section 2.1) the difference in mean soil bound was significant (P adj. = 0.01, 95% CI = 0.29, 2.15). The differences between the other cultivars were not significant (P = > 0.05).

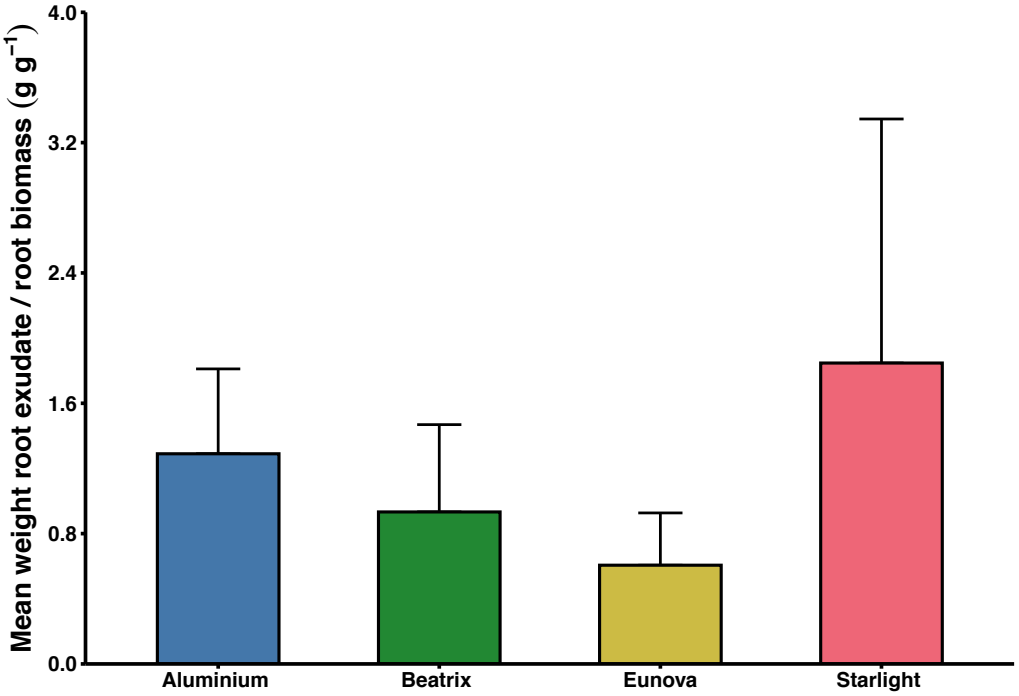

Figure. 5 Dry weight of high-molecular weight (HMW) root exudate per gram of fresh root biomass of Barley cultivars.

Barley cultivars (*Hordeum vulgare* L., cvs. Aluminium, Beatrix, Eunova and Starlight) were grown hydroponically in 9 L buckets, and the HMW fractions of root exudate isolated. The exudate (> 30 KDa) was lyophilised, dialysed against de-ionised water, and lyophilised again; this provided the dry weight of HMW root exudate. The total root biomass of all the plants in a bucket was recorded and gram of dry weight of HMW root exudate per gram of fresh root biomass was calculated. There was no significant difference between the gram of root exudate per gram of fresh root biomass (One-way ANOVA; $F = 1.22$, $P = > 0.05$).

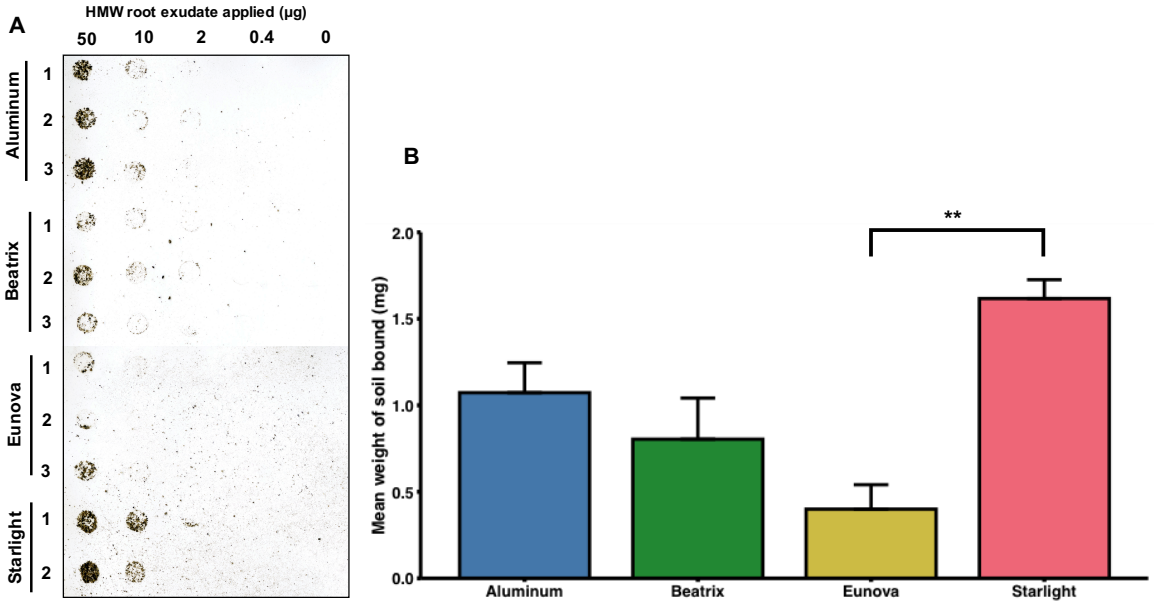

Figure. 6 Analysis of the soil-binding capacities of the high-molecular weight (HMW) root exudates of barley.

Barley cultivars (*Hordeum vulgare* L., cvs. Aluminium, Beatrix, Eunova and Starlight) were grown hydroponically in 9 L buckets, and their HMW fractions of root exudate isolated. For each cultivar three (two for Starlight) exudate samples were collected. **(A)** Representative image of nitrocellulose-based assay with 5 µL spots of exudate applied at 50 µg, 10 µg, 2 µg, and 0.4 µg. **(B)** Quantification of the mean amount of soil bound by the HMW exudate of each cultivar applied at 50 µg. Calculation used the calibration curve equation (Akhtar *et al*., 2018). Five to six plants were grown in each bucket and this formed one biological replicate. Data points are the means of three biological (Starlight n= 2) and three technical replicates. Error bars show standard error. ** = $P < 0.01$ when means were compared using a one-way-ANOVA and Tukey's Honestly significant different posthoc testing was applied.

3.2 A different set of polysaccharides are released from barley seedlings compared to plants grown hydroponically

To investigate the polysaccharide contents of exudates released by the barley genotypes at a younger stage of development than the plants growing in hydroponics, ten-day old seedlings root exudate were screened with MAbs by ELISA. It also allowed for a quantitative assessment of the polysaccharide epitopes present in plants at a similar age and developmental stage as those used in the nitrocellulose seedling printing (section 3.3). Seedling exudate collection provided a higher throughput method than hydroponics with plants only growing for 10 days as opposed to two weeks. This meant more plants could be screened in a shorter space of time. This investigation also allowed for some determination of the effect of the hydroponics and processing method on the root exudate and whether this caused changes in the epitope profiles detected.

3.2.1 The root exudate of barley seedlings contains xylan, xylogalacturonan, AGP and beta-glucan epitopes

Barley (cvs., Aluminium, Beatrix, Eunova and Starlight) seedling roots were left to exude in deionised water for four hours. The collected liquid was then analysed by ELISA with the same panel of 12 antibodies as in section 3.1.2 resulting in the heatmap in Figure 7. Whilst the epitopes that were present in the seedling exudate were mostly the same as the HMW exudate from hydroponics, the patterns of strength of the signals were different. Unlike the exudate from hydroponics the strongest epitope in the seedling exudate was that of LM6-M arabinan, and AGP signals (LM2, LM30) were also comparatively higher. Signals for the LM1 extensin epitope were reduced, and those of beta glucan 7E1:B11 epitope were considerably stronger compared to that collected from hydroponics. A notable difference was the signal strength of the LM8 xylogalacturonan epitope which was high in the seedling exudate for all cultivars but was not present in the processed HMW exudate from hydroponics. Likewise, it was not found in the wheat root exudate from hydroponics (Galloway *et al.*, 2020).

3.2.2 Root length but not seedling weight varied between of barley cultivars

The barley seedlings were germinated on agar plates for 10 days and were typified by an extended coleoptile, a long radicle and several seminal roots. Analysis of the seedling growth was measured by whole fresh seedling biomass and length of the longest root of each seedling. The results are presented in Figure 8. The decision to measure whole seedling mass in contrast to removing and weighing the roots was made so the seedling could be reused in nitrocellulose printing experiments. No Starlight seedlings were measured for these traits due to insufficient seed stock. Differences in the effect of cultivar on mean seedling weight were tested for statistical significance and it was found that none existed (One-way ANOVA; $F = 1.26$, $P = > 0.05$). However, cultivar did influence length of the longest root length for a least two groups (One-way ANOVA; $F = 15.23$, $P = < 0.001$). Tukey's HSD test found that the average longest root length was significantly longer in Beatrix than Aluminium (P adj. = <0.001, 95% C.I. = 2.01, 5.22) and in Beatrix compared to Eunova (P adj. = 0.01, 95% C.I. = -2.17, -3.67).

		Aluminum		Beatrix		Eunova		Starlight		Scale
Antigen	**Antibody**	Mean	SD	Mean	SD	Mean	SD	Mean	SD	2
Heteroxylan	LM11	0.273	0.254	0.309	0.289	0.366	0.300	0.004	0.008	1.5
	LM27	0.381	0.347	0.420	0.257	0.410	0.263	0.042	0.039	1
Xylogucan	LM25	1.190	0.246	1.177	0.307	1.359	0.326	1.148	0.223	0.5
Heteromannan	LM22	0.290	0.321	0.114	0.192	0.069	0.102	0.000	0.001	0.1
Arabinan	LM6M	1.625	0.248	1.659	0.308	1.601	0.366	1.324	0.243	
Xylogalactoronan	LM8	0.953	0.369	0.523	0.364	0.821	0.454	0.432	0.272	
AGP	LM2	0.541	0.371	0.849	0.449	0.755	0.494	0.384	0.601	
	LM30	0.882	0.398	1.008	0.383	0.796	0.625	0.251	0.140	
Extensin	LM1	0.103	0.066	0.101	0.062	0.088	0.064	0.051	0.071	
Beta-glucan	JIM6	0.068	0.049	0.134	0.111	0.285	0.507	0.005	0.010	
	10H2	0.153	0.159	0.064	0.141	0.059	0.119	0.007	0.015	
	7E1/B11	1.288	0.320	0.843	0.328	0.767	0.539	0.432	0.583	

Figure. 7 Heatmap comparison of the polysaccharide epitopes detected per unit volume of the collected seedling root exudate of barley cultivars.

Barley (*Hordeum vulgare* L., cvs. Aluminium, Beatrix, Eunova and Starlight) seedlings were germinated for 10 days and their root systems left to exude in 5.5 ml of de-ionised water for 4 hours. For each cultivar exudate samples were collected from multiple seedlings and then individually analysed by indirect ELISA. Values shown are from wells coated with a 1 in 5 dilution of the collected exudate. Values are absorbance at 450 nm representing the means of multiple biological replicates (Aluminium n= 15, Beatrix n= 26, Eunova n= 20, Starlight n = 6). Heatmap scale gradient shown on the right. SD; standard deviation, AGP; Arabinogalactan protein

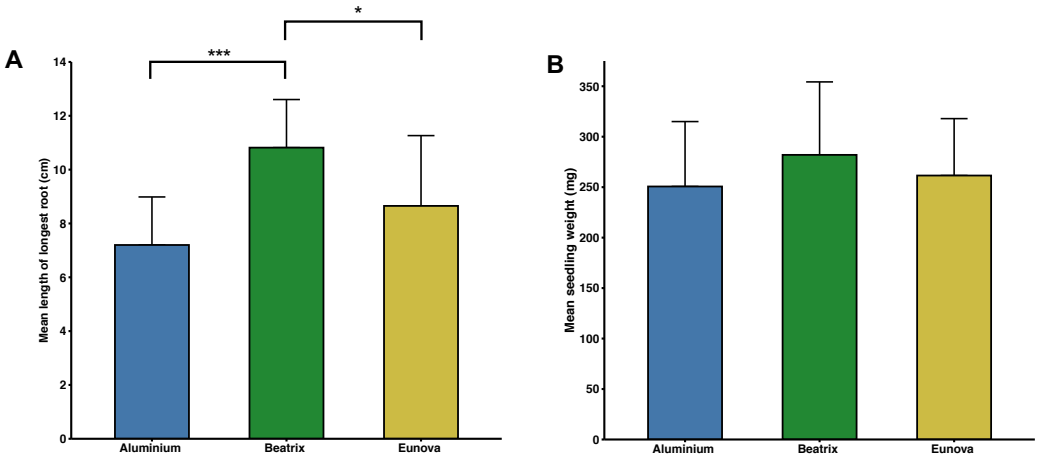

Figure. 8 Mean longest root lengths and fresh weight of seedlings of barley cultivars

Barley cultivars (*Hordeum vulgare* L., cvs. Aluminium, Beatrix, and Eunova) were grown on agar plates for 10-days, then left to exude in 5.5 mL of de-ionised water for four hours. (A) The roots of each seedling where then extended the longest root identified and then measured. Significance codes; *= P < 0.05; ***= P< 0.001 after means were compared using a one-way-ANOVA and Tukey's Honestly significant different post hoc testing was applied. (B) The total root and shoot biomass (fresh weight of each seedling) was measured and recorded. There was no significant difference between the fresh weight of each seedling. Data points represent the means of multiple biological replicates (Aluminium n= 18, Beatrix n= 23, Eunova n= 23). Error bars show standard deviation.

3.3 Barley seedlings release polysaccharide epitopes from along their root axis in a similar manner between cultivars

In view of the accumulated literature on root tip mucilage but the limited understanding of polysaccharides released from other areas of the root, a nitrocellulose-based seedling printing technique was initiated to determine which region of the root the majority of polysaccharides were released from in the barley seedlings. The subsequent sets of prints (Figs. 9-12) show that although the release of different epitopes is contrasting, they are all released from along the length of the root axis. The LM8 xylogalacturonan epitope shows the weakest release, and has previously has been associated with shed root cap cells and mucilage at root tips (Willats *et al.*, 2004; Durand *et al.*, 2009; Cannesan *et al.*, 2012). Here the epitope is seen to be released from along the root's length. The release of the 7E1:B11 and AGP (LM30 and LM2) epitopes were smudgy and smeared across the sheet. Whereas the xylan LM27 epitope is comparatively cleaner and better defined. Prints developed with the LM5 galactan antibody acted as a negative control, as it had not previously been detected in the wider screen of seedling exudate (section 3.2.3). The lack of discernible print with LM5 staining, which is potentially indicative of galactose residues on the rhamnogalacturonan-I (Willats *et al*., 1998; Cornuault *et al*., 2018) increases the likelihood the LM6-M epitope is associated with arabinose residues on AGPs and not from pectic polysaccharides. Differences in the release of polysaccharides between cultivars is less clear, the release LM27 and 7E1:B11 epitopes are broadly similar between Aluminium, Eunova, and Beatrix seedlings but comparatively weaker from Starlight seedlings. On Beatrix seedling prints the release of the LM30 epitope smears away from the root, which is not seen with this epitope for the other cultivars. Between cultivars Beatrix also gives the faintest prints for the LM8 epitope, it appears its release is weaker from this cultivar. The printing process is sensitive to moisture present on the nitrocellulose sheet, after this was discovered care was taken to apply the same amount of de-ionised water to each sheet and make sure no surface water remained. Large gaps in the prints indicate where the seedling has lifted up off the nitrocellulose and does not indicate lack of exudation.

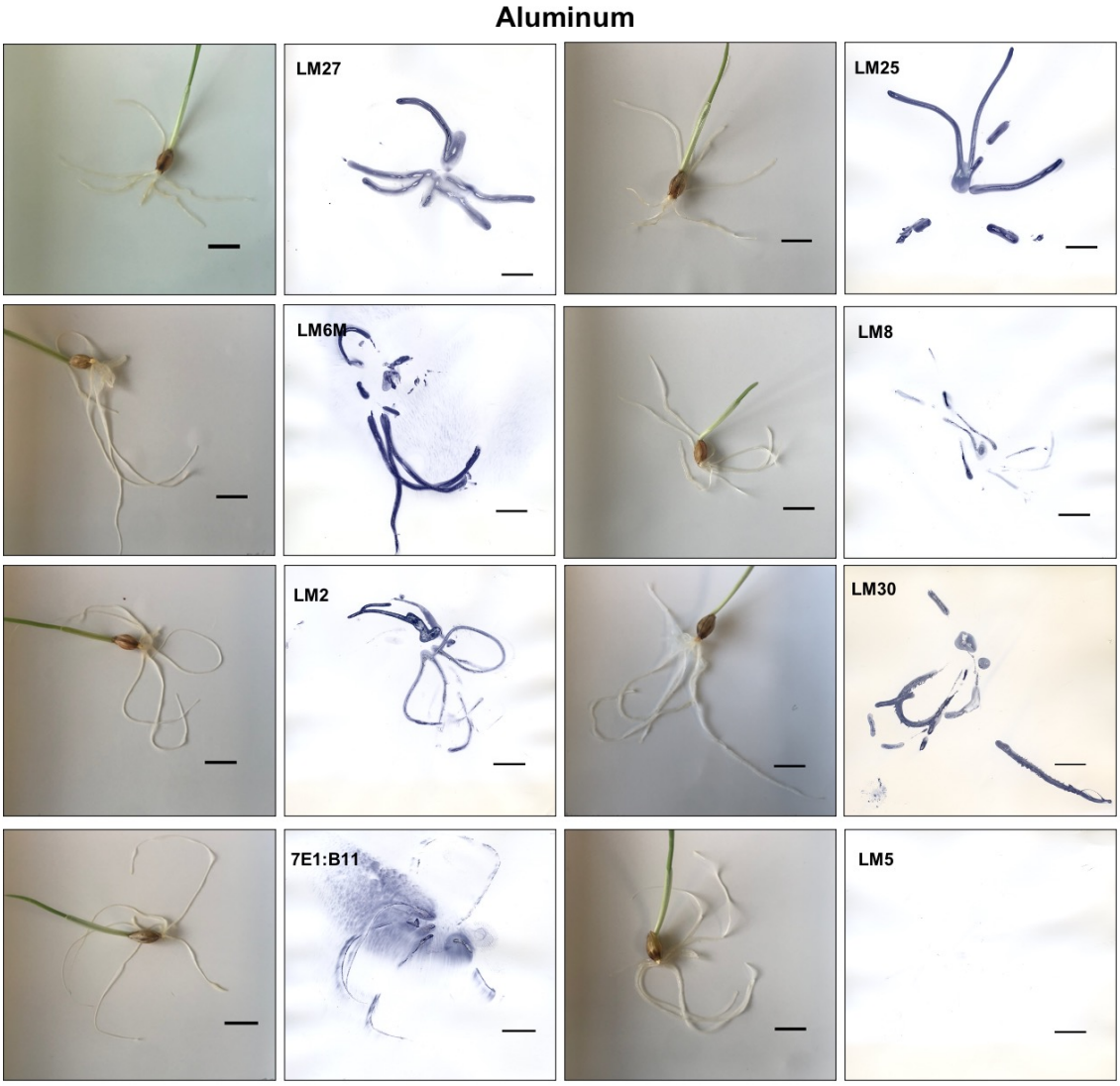

Figure. 9 Barley seedling root nitrocellulose prints tracking the release of polysaccharide epitopes.

Paired images of prints of 10-day old barley (*Hordeum vulgare* L. cv. Aluminium) seedlings placed on nitrocellulose sheets for one hour and photographs of the seedling on the nitrocellulose *in situ.* Seedlings were then removed and the sheets left to dry overnight. Sheets were then probed with monoclonal antibodies. LM27, heteroxylan; LM25, xyloglucan; LM8, xylogalacturonan; LM6-M, arabinan; LM2 and LM30, arabinogalactan protein (AGP); 7E1:B11, beta-glucan; LM5, galactan (negative control). Each image representative of at least two prints. Scale bars 10 mm.

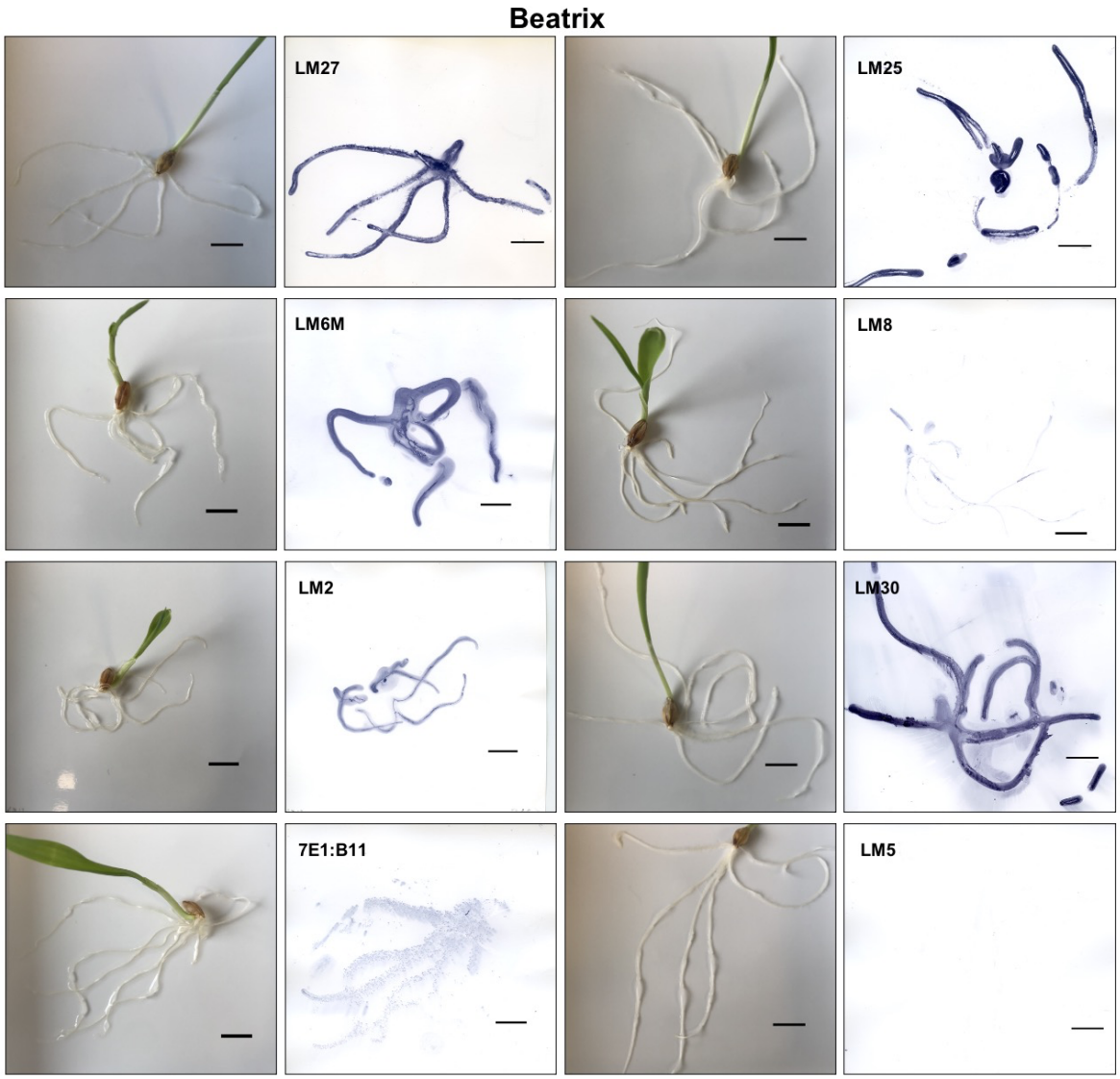

Figure. 10 Barley seedling root nitrocellulose prints tracking the release of polysaccharide epitopes.

Paired images of prints of 10-day old barley (*Hordeum vulgare* L. cv. Beatrix) seedlings placed on nitrocellulose sheets for one hour and photographs of the seedling on the nitrocellulose *in situ.* Seedlings were then removed and the sheets left to dry overnight. Sheets were then probed with monoclonal antibodies. LM27, heteroxylan; LM25, xyloglucan; LM8, xylogalacturonan; LM6-M, arabinan; LM2 and LM30, arabinogalactan protein (AGP); 7E1:B11, beta-glucan; LM5, galactan (negative control). Each image representative of at least two prints. Scale bars 10 mm.

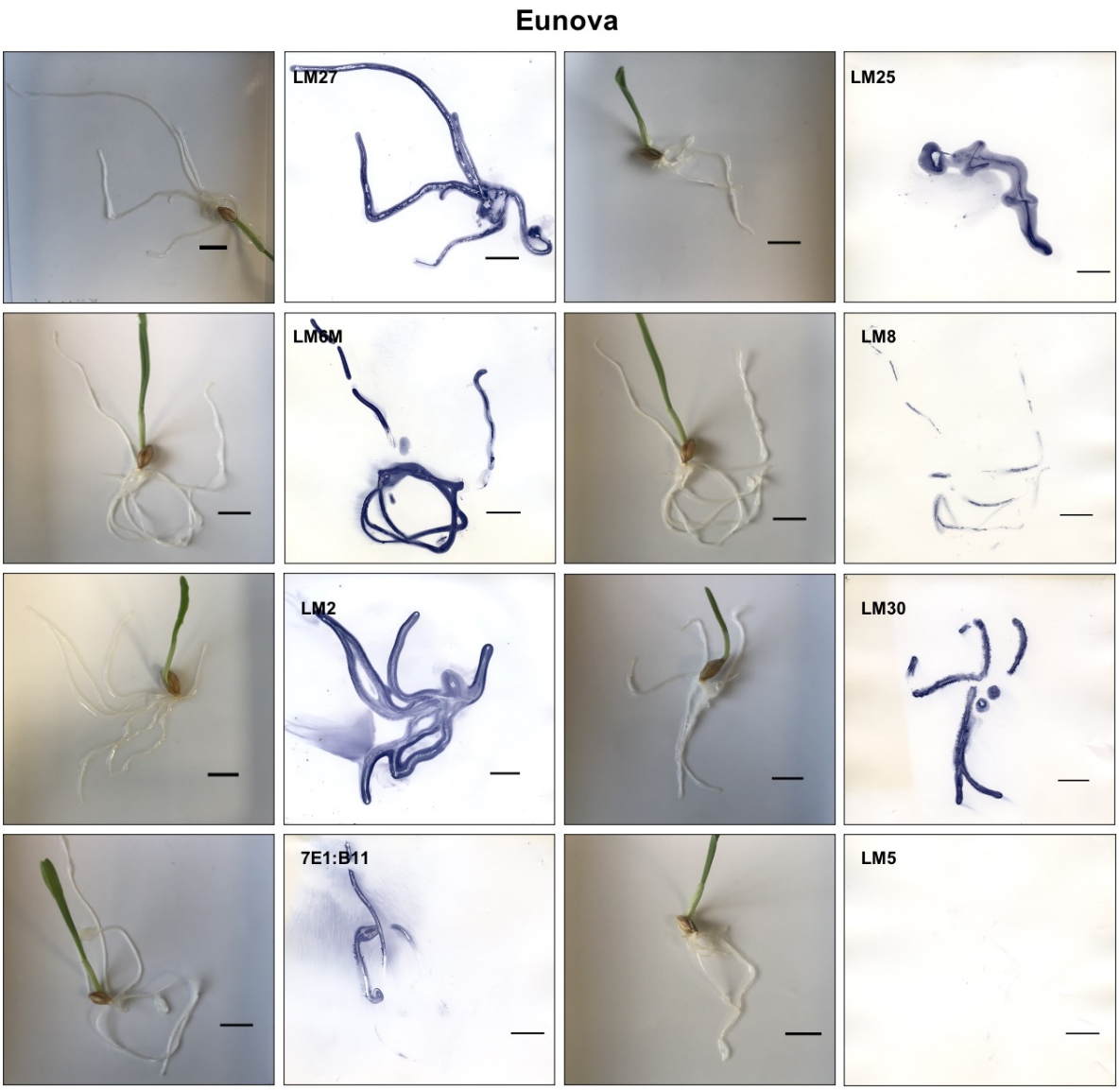

Figure. 11 Barley seedling root nitrocellulose prints tracking the release of polysaccharide epitopes.

Paired images of prints of 10-day old barley (*Hordeum vulgare* L. cv. Eunova*)* seedlings placed on nitrocellulose sheets for one hour and photographs of the seedling on the nitrocellulose *in situ.* Seedlings were then removed and the sheets left to dry overnight. Sheets were then probed monoclonal antibodies. LM27, heteroxylan; LM25, xyloglucan; LM8, xylogalacturonan; LM6-M, arabinan; LM2 and LM30, arabinogalactan protein (AGP); 7E1:B11, beta-glucan; LM5, galactan (negative control). Each image representative of at least two prints. Scale bars 10 mm.

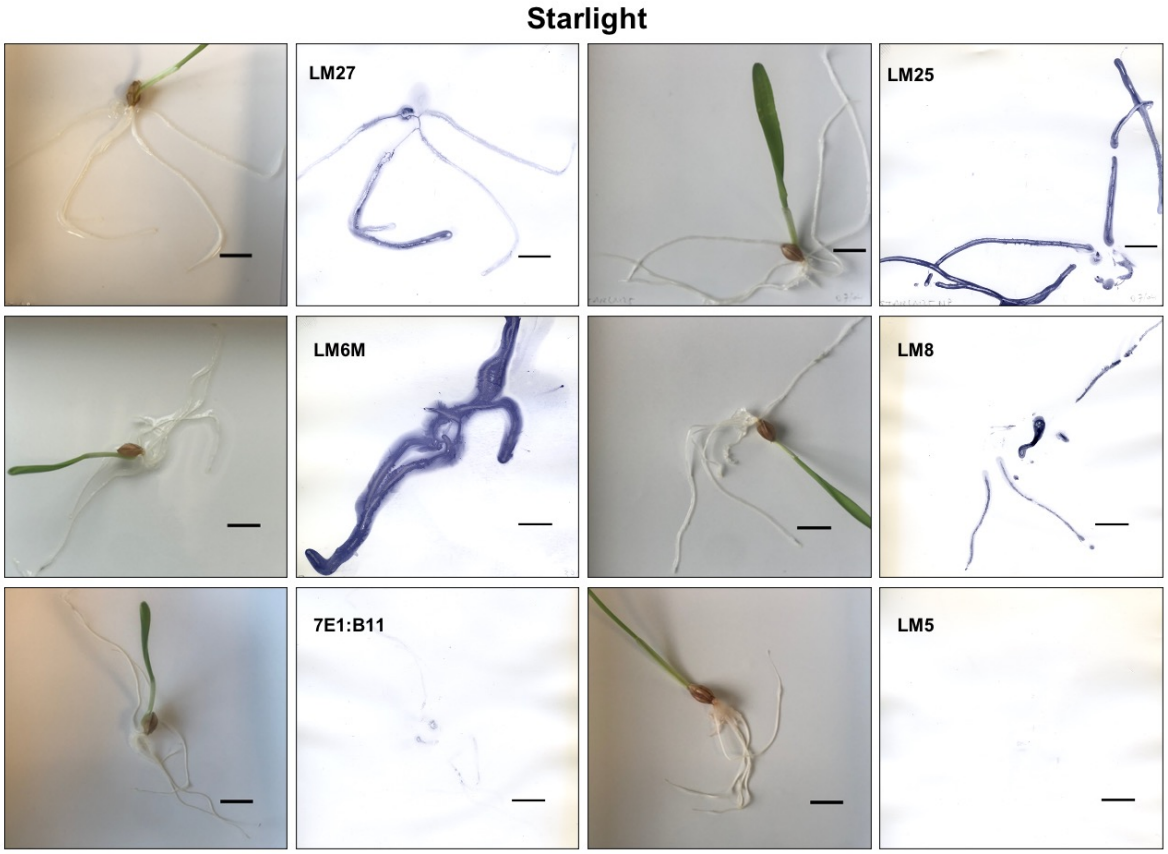

Figure. 12 Barley seedling root nitrocellulose prints tracking the release of polysaccharide epitopes.

Paired images of prints of 10-day old barley (*Hordeum vulgare* L. cv. Starlight) seedlings placed on nitrocellulose sheets for one hour and photographs of the seedling on the nitrocellulose *in situ.* Seedlings were then removed and the sheets left to dry overnight. Sheets were then probed with monoclonal antibodies. LM27, heteroxylan; LM25, xyloglucan; LM8, xylogalacturonan; LM6-M, arabinan; 7E1:B11, beta-glucan; LM5, galactan (negative control). Each image representative of at least two prints. Scale bars 10 mm.

3.4. The root exudate of barley plants in soil shares similarities with plants grown under different systems

Thus far investigations focused on root exudate collection methods from plants suspended in liquid, these however are not representative of growth in the soil matrix. To examine the contrasting polysaccharides profiles between soil and liquid medium grown plants, a suction lysimeter was used to try and extract root exudate directly from soil. The technique was analogous to soil washing, barley plants grew in sand-soil mixture and after a period of watering, the water from around the root containing any soluble exudate was collected to be analysed. The collected exudate was analysed by ELISA and probed with sixteen MAbs (Fig.13). Epitope signals were much weaker than those of either the processed HMW exudate or the seedling incubations. However, the strongest signals came from the LM6-M epitope which also gave the highest signals in the seedling exudate (Fig.7) This suggests that rather than containing fewer epitopes instead the lysimeter collected exudate solution is far more dilute than that of the other collection methods. A non-plant negative control to test for any cell wall related polysaccharide epitopes present in the soil or from associated microbes showed only the 10H2 beta-glucan epitope.

		Aluminum		Beatrix		Eunova		No plant control		Scale
Antigen	Antibody	Mean	SD	Mean	SD	Mean	SD	Mean	SD	2
Heteroxylan	**LM11**	0.032	0.056	0.004	0.005	0.016	0.021	0.009	0.010	1.5
	LM27	0.046	0.080	0.000	0.000	0.000	0.000	0.000	0.010	1
Xylogucan	**LM25**	0.052	0.069	0.011	0.018	0.072	0.133	0.002	0.005	0.5
Heteromannan	**LM22**	0.040	0.053	0.001	0.001	0.015	0.013	0.046	0.008	0.1
Galactan	**LM5**	0.032	0.055	0.001	0.002	0.000	0.000	0.000	0.003	
Arabinan	**LM6M**	0.103	0.160	0.114	0.159	0.340	0.315	0.000	0.005	
Homogalactoronan	**LM19**	0.055	0.078	0.006	0.005	0.012	0.022	0.000	0.011	
	LM20	0.024	0.031	0.008	0.005	0.017	0.026	0.006	0.005	
Xylogalactoronan	**LM8**	0.036	0.045	0.011	0.019	0.032	0.012	0.014	0.001	
AGP	**LM2**	0.025	0.043	0.001	0.001	0.005	0.009	0.000	0.010	
	LM30	0.032	0.044	0.004	0.003	0.006	0.012	0.008	0.004	
	JIM13	0.163	0.183	0.010	0.008	0.009	0.008	0.000	0.008	
Extensin	**LM1**	0.029	0.043	0.001	0.001	0.010	0.009	0.010	0.006	
Beta-glucan	**JIM6**	0.058	0.050	0.009	0.008	0.010	0.007	0.010	0.005	
	10H2	0.218	0.166	0.017	0.022	0.015	0.011	0.553	0.056	
	7E1:B11	0.116	0.023	0.024	0.014	0.036	0.027	0.063	0.010	

Figure. 13 Heatmap of the polysaccharide epitopes detected in the suction-lysimeter collected root exudate of barley plants grown in soil.

Barley (*Hordeum vulgare* L., cvs Aluminium, Beatrix, and Eunova) seedlings were grown in pots in a sand/sieved soil mixture for two weeks. A soil suction lysimeter was added to collect soluble exudates. For each cultivar exudate samples were collected from multiple plant pots and then individually analysed by indirect ELISA. Values shown are from wells coated with a 1 in 5 dilution of the collected exudate. Values are absorbance at 450 nm representing the means of multiple biological replicates (Aluminium n= 3, Beatrix n= 4, Eunova n= 4). Heatmap scale gradient shown on the right. SD; standard deviation, AGP; Arabinogalactan-protein

3.5 Barley cultivars varied in rhizosheath size but not root hair length

To compare the rhizosheath size of the barley genotypes they were grown in a 50:50 sand-soil mixture for two weeks and screened for rhizosheath weight using the method in Section 2.10. In order to resolve differences in the effect of cultivar on rhizosheath weight, root dry biomass and rhizosheath per root weight a one-way ANOVA was used and found no significance ($P > 0.05$) in any factor between the groups.

This was complemented by data provided by the James Hutton Institute who performed a rhizosheath screen of ten-day old plants grown individually. The lengths of root hairs were also provided; for each genotype ten plants had ten root hairs measured. A one-way ANOVA was performed to compare the effect of cultivar on rhizosheath weight and revealed that a statistically significant difference existed in rhizosheath weight between at least two groups ($F = 8.74$, $P = < 0.001$). Tukey's HSD Test found that the mean rhizosheath weight was significantly different between Aluminium and Starlight (P adj. = < 0.01, 95% CI = 0.77, 2.89), Beatrix and Starlight (P adj. = < 0.001, 95% CI =0.76, 2.89) and Eunova and Starlight (P adj. = < 0.05, 95% CI = -0.02, 4.24). Similarly, the statistically significant difference existed in dry root biomass between at least two cultivars (One-way ANOVA; $F = 7.46$, $P = < 0.01$), and Tukey's HSD of multiple comparisons revealed these groups to be Beatrix and Starlight (P adj. = < 0.01, 95% CI = -0.04, -0.01), Beatrix and Eunova (P adj. = < 0.05, 95% CI = -0.69, -0.004). A gram for gram comparison of rhizosheath weight per dry root biomass provides a comparison considering for differences in the root growth between cultivars. Although its effectiveness here was hindered by only one replicate for the barley cultivar Eunova being provided. However, rhizosheath per root weight was significantly affected by barley cultivar (One-way ANOVA; $F = 23.04$, $P = < 0.001$). Multiple comparison testing with Tukey's HSD showed that mean rhizosheath per root weight was significantly different between Starlight and Aluminium (P adj. = < 0.001, 95% CI = 76.77, 214.41), Starlight and Beatrix (P adj. = < 0.001, 95% CI = 93.63, 212.84). Whilst Eunova's rhizosheath per root weight was significantly larger than both Aluminium and Beatrix (P adj. = < 0.05) the lack of replicates undermines reliability of these assertions. There was no significant difference in mean root hair length between the cultivars (One-way ANOVA; $F = 0.263$, $P = > 0.05$).

Table.4 Comparison of data from rhizosheath screens, rhizosheath per root weight and mean root hair length of barley cultivars

Line	Rhizosheath weight (g)	SD	Dry root biomass (g)	SD	Rhizosheath per root (g g^{-1} root dry weight)	SD		
(A) Data collected at University of Leeds								
Aluminium	2.57	1.48	0.03	0.02	89.45	32.54		
Beatrix	2.00	1.90	0.03	0.01	56.57	45.72		
Eunova	3.03	1.69	0.04	0.01	90.32	47.16		
(B) Data provided by the James Hutton Institute								
							Root hair length (mm)	SD
Aluminium	2.51 [b]	0.62	0.04	0.01	56.996 [c,e]	13.49	-	-
Beatrix	2.251 [c]	0.78	0.0455 [b,d]	0.01	49.35 [c,e]	16.65	1.41	0.39
Eunova	1.97 [a]	-	0.01	-	218.89	-	1.55	0.53
Starlight	4.08	0.47	0.02	0.01	202.59	73.63	1.46	0.43

Table. 4 Comparison of data from rhizosheath screens, rhizosheath per root weight and mean root hair length of barley cultivars.

(A) Barley cultivars (*Hordeum vulgare* L., cvs Aluminium, Beatrix, Eunova and Starlight) were grown five to six seedlings per pot in a sand/sieved soil mixture for two weeks, they were then excavated and the rhizosheath weight measured. Data points are the means of multiple replicates (Aluminium n = 10 Beatrix n = 12 Eunova n = 11) There was no significant difference between cultivars for rhizosheath weight, root dry biomass and rhizosheath per root weight. **(B)** Data provided by the James Hutton Institute, barley cultivars germinated on agar plates and then left to grow in soil for a further seven days. Data points are the means of five replicates (Eunova n= 1). Root hairs values average of 100 root hairs from ten different plants. No data was provided for Aluminium. There was no significant difference between the effect of cultivar on mean root hair length. Multiple one-way-ANOVAs were used compared the effect of cultivar on rhizosheath weight, dry root biomass, and rhizosheath per root weight. For the data collected at the University of Leeds there was no significant difference in the effect of cultivar on either rhizosheath weight ($F= 1.03$, $P > 0.05$), dry root biomass ($F= 0.56$, $P > 0.05$), or rhizosheath per root weight ($F= 2.35$, $P > 0.05$). For data provided by James Hutton Institute there was significant difference between at least two groups effect of cultivar on either rhizosheath weight ($F= 8.74$, $P > 0.05$), dry root biomass ($F= 7.46$, $P > 0.05$), or rhizosheath per root weight ($F= 2.32$, $P > 0.05$). After means were compared using Tukey's Honestly significant different test [a] = P adj < 0.05 compared to Starlight; [b] = P adj.< 0.01 compared to Starlight ; [c] = P adj < 0.001 compared to Starlight; [d] = P < 0.5 compared to Eunova ; [e] = P adj < 0.01 compared to Eunova.

3.6 Root surfaces of barley cultivars show an abundance of beta-glucan and AGP epitopes

Whilst analysis by ELISA gives us a detailed profile of the polysaccharide epitopes present in the exudate, all spatial localization is lost – it is not known from where the on root the epitopes originate. Nitrocellulose tissue printing helped to identify the spatial release of mobile exudates. But there is a possibility that some exudates did not move away into the surrounding environment but were retained at the root surface. The labelling of whole root segments provides an *in situ* visualisation of these polysaccharides epitopes (Fig.14). Four MAbs were chosen, LM6-M, because of its high levels in the barley exudate which are unseen in other cereals (Galloway *et al.*, 2020). LM8, to provide further analysis of this epitopes spatial release. LM2, which has known associations with root hairs (Marzec *et al.*, 2015). The novel antibody 7E1:B11, in order to observe its potential presence at barley root surfaces for the first time. Labelling with LM8 antibody was negative, equivalent to no antibody being present, it was therefore used as a control. The non-binding of this primary antibody (LM8) presents a good alternative to a no antibody control as even with a primary antibody is present but there is no antigen binding.

The LM8 epitope was not detected at any level in most of the cultivars in ELISA analysis of the HMW exudate (Fig.3), it was however detected abundantly in the analysis of seedling exudate (Fig.7) and on nitrocellulose seedling prints it was released from along the root axes (Figs.9-12). Previously the epitope has been seen associated with root tips. To observe if the LM8 epitope was at root apices on hydroponically grown plants, but somehow being lost in processing and ELISA analysis, surfaces ~1 cm segments of the root apices were probed with the LM8 antibody, apart from on one replicate where it was detected at low levels (Fig.15ii) the LM8 epitope was not found at the root tips of either of the analysed cultivars.

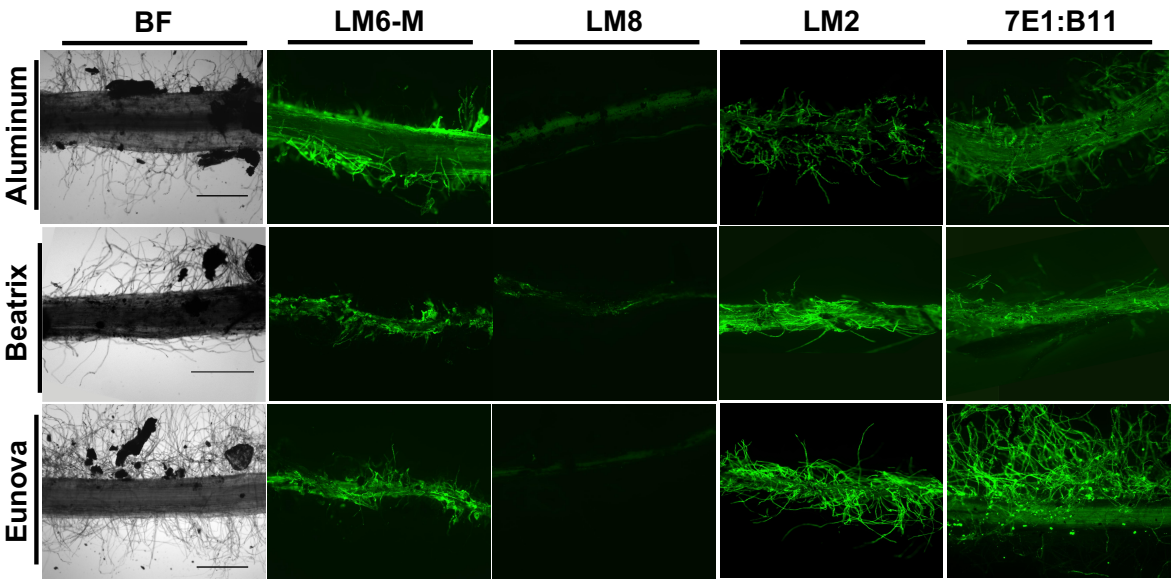

Figure. 14 Comparative micrographs of whole mount immunofluorescence labelling of barley root surfaces.

Barley (*Hordeum vulgare* L., cvs. Aluminium, Beatrix, and Eunova) seedlings were grown in pots in a sand/sieved soil mixture for two weeks. Root segments (~ 1 cm) were then probed with monoclonal antibodies: LM6-M arabinan, LM8 xylogalacturonan, LM2 AGP, 7E1:B11 ß-glucan. Images paired with a representative bright field (BF) micrograph. Labelling indicated both β-glucan and AGP epitopes abundant at root hair surfaces and non-binding of a xylogalacturonan epitope. Each image is representative of micrographs of three different root segments. Root segments of ~ 1 cm in length were taken 3 cm up from the root apex**.** Contrast on some images has been enhanced to improve clarity. Scale bar = 500 µm

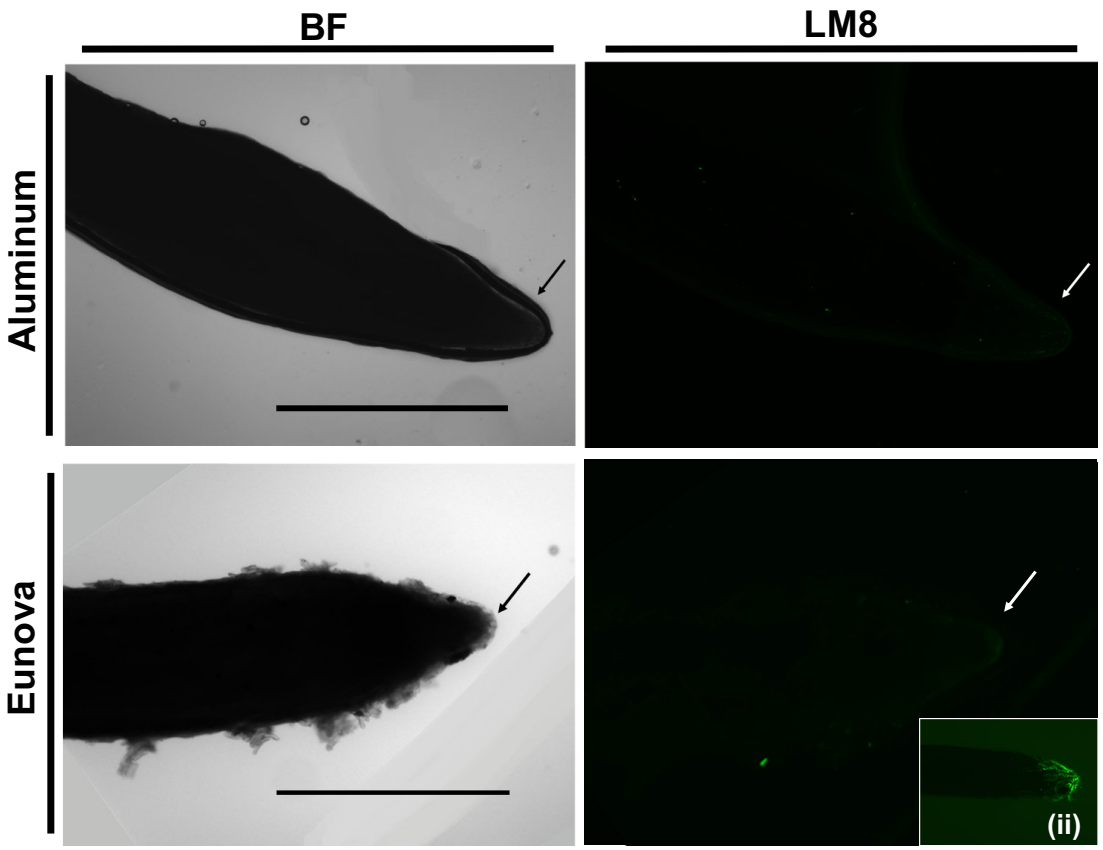

Figure. 15 Comparative micrographs of whole mount immunofluorescence labelling of barley root apices.

Barley (*Hordeum vulgare* L., cvs. Aluminium and Eunova) plants were were grown hydroponically for two weeks. Root segments ~ 1cm up from the root apex were then probed with the monoclonal antibody LM8 (xylogalacturonan). Images indicate non-binding of the LM8 epitope which has previously been associated with the root apices (Willats *et al.*, 2004). Each image is representative of micrographs of two different root apices. (ii) A lone instance of low level detection of the LM8 epitope of the tip of a Eunova root. Arrows indicate root apices. Scale bar = 500 µm

Chapter 4
Discussion

The purpose of this investigation was to identify the polysaccharide factors released from roots and explore whether they could explain differences in rhizosheath size across a range of barley cultivars. The key results are summarised in Fig.16. The work described here has determined the polysaccharide epitope profiles of the root exudate of barley genotypes and characterised the spatial release of these glycan epitopes from along the root axis. It also established that certain AGP associated epitopes and a new beta-glucan epitope are presented on the root hairs of soil grown barley plants. This study also discovered that there is a possible carbon allocation trade-off between root growth and release of soil binding HMW exudate between barley genotypes. These could represent different strategies to form a robust root system between the cultivars. As well as that soil binding capacity of the high molecular weight (HMW) components of exudate is linked to the rhizosheath weight of barley roots.

One of the most striking results was the large variation in epitope signals between the root exudates of seedlings within the same cultivar, emphasised by the high standard deviations of absorbance values (Fig.7). A possible factor in this that the exudate is collected from seedlings at an early stage of growth. For those epitopes known to be associated with root hairs, for example LM2 (Fig.14) it could be variation in the root hair growth, as a consequence of the difference in the developmental stage of the seedlings resulting in less surface area for an epitope to be presented from. However, whilst this may explain the variation for those epitopes, it also persists for epitopes not linked with root hairs e.g. LM8 (Fig.14). This intra-cultivar variation could be as a result of the phenotypic plasticity of exudate release, and the ability for a seedling to negotiate different circumstances. This suggestion poses two possibilities; (1) growth differences on the agar plate mean the germinating seedling is already exuding different amounts of polysaccharides when it is incubated in water or (2) the exudation differences begin after it is placed in the water. In either case, the conditions of germination and growth were highly controlled to mitigate against potential differences. On the other hand, another explanation could be a change in solubility of the polysaccharides leading to them precipitating out of solution (Guo *et al.*, 2017). They would then be lost when the solution is used to coat ELISA plates. Although there were no visible

signs of this. Regardless, a way to test if this was the case would be to rinse the bottle with potassium hydroxide or another basic extractant (Seymour *et al.*, 1990; Pattathil *et al.*, 2012) and then use this solution to coat the ELISA wells. Despite this, the mechanism influencing either of these explanations are unknown.

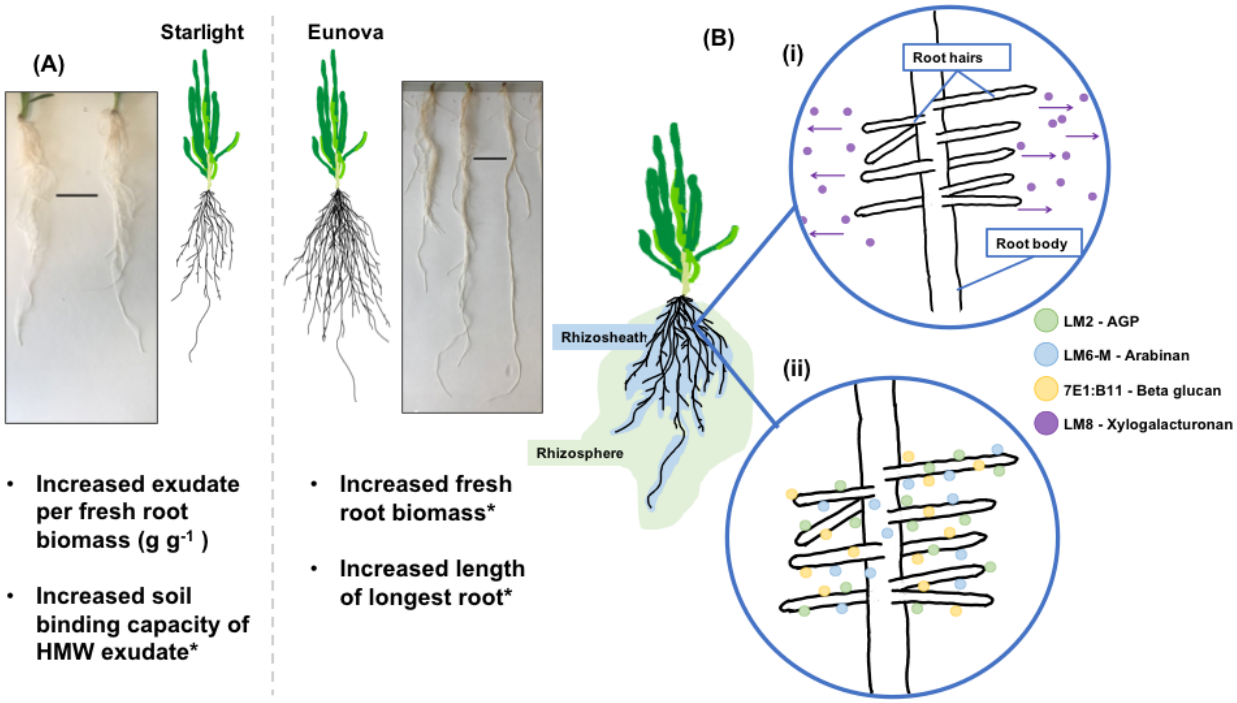

Figure. 16 A schematic overview of the of key results of the investigation into barley (*Hordeum vulgare* L.) rhizosheaths and polysaccharide root exudates.

(A) Comparison of Eunova and Starlight barley genotypes. These two cultivars showed large differences in root system growth and in the release of HMW exudate. The contrast in these two traits between the two genotypes suggests that there is a trade-off in carbon allocation by the plant between root growth and HMW exudation. * = Genotypes showed significant difference between these traits ($P < 0.05$ when means were compared using a one-way-ANOVA and Tukey's Honestly significant different post hoc testing was applied). Scale bar = 5 cm. (Bi) The pattern of the LM8 (xylogalacturonan) epitope's release from along the root axes as detected by the seedling prints on nitrocellulose sheets. The LM8 epitope's presence here, but not a root surfaces, suggests it is on a molecule that moves away from the root. (Bii) Immunofluorescence microscopy established the abundance of AGP epitopes and a beta-glucan epitope at root hair surfaces. With these results, it is proposed that groups of glycan epitopes have distinct functions; presentation on root hairs is associated with soil binding, but the release of the LM8 epitope provides another unknown function for the root system.

4. 1 Exudation, soil binding and rhizosheath size

Rhizosheath formation relies on the joint action of root hairs and adhesive root exudates (Moreno-Espindola *et al.*, 2007; Brown *et al.*, 2017; Galloway *et al.*, 2020). However, previous studies have shown, that unlike wheat, barley rhizosheaths were not affected by root hair length (Delhaize *et al*., 2012; George *et al.*, 2014). This highlights other traits as important in barley rhizosheath formation, notably root exudation. Of the barley cultivars screened Starlight was found to have the largest rhizosheath and the greatest rhizosheath per root weight (Table.4b). Between the cultivars there was no significant variation in root hair length (Table.4b). Although, there was a substantial difference in the amount of soil the HMW exudates could bind (Section 3.1.5) the HMW exudate of Starlight bound the most soil compared to the other genotypes, and significantly more so than the HMW exudate of Eunova (Fig.6). Therefore, in this report a major determinant of rhizosheath weight in between these two barley genotypes was the soil binding capacity of the HMW compounds in root exudates. This partially supports the primary question of this investigation, as Starlight is a large rhizosheath genotype and in a per weight comparison the HMW exudate released by its root system adhered the most soil. However there was only one other genotype with which this comparison was statistically significant, the other large rhizosheath cultivars (Eunova). Further rhizosheath screens help and would elucidate whether these are both truly cultivars which form large rhizosheaths. After this was resolved and if Eunova was correctly identified as a large rhizosheath line, then it could be that there are a number of way to form a robust rhizosheath, possibly linked to the comparative extensive root growth of Eunova (Fig. 4).

The significance of HMW exudate in in rhizosheath formation runs contrary to other work in barley which found the relative contribution of root hairs greater than exudation (Burak *et al*., 2021). It could still be possible that root hair growth was responsible for differences in rhizosheath weight between these barley genotypes. In the study in Table.4b root hair length was the only trait that was measured, another trait such as root hair density may have differed between the barley lines and further examination would be useful to explore. It was also the case that the experimental designs of the two investigations were organised with different questions in mind. Burak *et al*., (2021) compared a root hairless mutant (brb) with its wild type counterpart, whereas the genotypes used in this study did not differ in root hair length. It is therefore no wholly unsurprising that the contributions of the

root hairs in rhizosheath formation were found to be far less in this report than in the published work. A consequence of root hair surfaces importance for the presentation of certain epitopes in exudate (Fig.14) would be that factors decrease root hair length and density such as soil acidity (Haling *et al.*, 2010a; Haling *et al.*, 2010b) would then not only affect the rhizosheath by reducing the ability for mechanical entrapment of soil particles but would also affect to the action of exudates at the root-soil interface.

The process of rhizodeposition translocates a significant amount of carbon from the plant into surrounding soil, the amount and composition of rhizodeposits varies depending on the plant species, microorganisms present, plant age and nutrient availability (Hütsch *et al.*, 2002; Nguyen, 2003; Jones *et al.*, 2004). How a plant allocates carbon can be thought of in economic terms, with one form of carbon usage incurring an opportunity cost on the others (Lynch & Ho, 2005). Starlight had the smallest root system growth of all the genotypes, its root biomass was 301% less and the length of its longest roots 71% shorter than that of Eunova (Fig.4). Despite this, Starlight released the most HMW exudate per gram of root biomass (Fig.5), HMW exudate that had the greatest soil binding potential of the all the barley genotypes (Fig.6). The comparative negative correlation between these traits for the two genotypes suggests that there is a trade-off in carbon allocation by the plant between root growth and HMW exudation, and specifically those exudates with a high soil binding capability. Starlight and Eunova demonstrate the extremes in this carbon trade-off, whilst Aluminium and Beatrix represent intermediates. The implication is that these differences in root growth and exudation are genotypic as the plants were grown under the same conditions, with no limiting resources. There are multiple strategies for a plant to cope with drought stress (Henry *et al.*, 2012). In a variety of plant species, extensive root growth and increased rooting depth, in response to drought, help the plant to explore greater volumes of soil to try increase water uptake (Buwalda, 1993; Asch *et al.*, 2005; Ji *et al.*, 2012). Greater exudation of carbon by the root system has also been observed in drought stressed crops (Henry *et al.*, 2007). The differences in root growth and exudation phenotypes between these lines could relate to the plants how they differentially allocate fixed carbon to form an efficient root system for resource capture. To see if these the traits of root system size and soil-binding HMW exudation are linked a hybrid cross of Eunova and Starlight and analysis of the progeny's root length, root biomass and exudation could be performed. A greater number of replicates would also enhance the ability to assess if the greater root system growth was significant.

All the genotypes displayed strong signals for the xyloglucan LM25 epitope, and it was released consistently from along the root axes in the seedlings. Xyloglucan effectiveness in aggregating soil particles has been established (Galloway *et al.*, 2018). The LM25 epitope's detection in the seedling and HMW exudate was at similar levels across the range of cultivars. Whilst this xyloglucan epitope is likely involved in soil particle aggregation in the soil binding assay (and the thus rhizosheaths) of the genotypes, differences in the levels of its release didn't appear to underpin differences in rhizosheath weight between the cultivars. Nevertheless, different forms of the xyloglucan epitope in root exudate have been discovered. Anion-exchange chromatography resolved two forms of the xyloglucan antigen, an acidic and a neutral fraction and application of the soil binding assay ascertained that it was the acidic form of xyloglucan, that was the better soil adhesive (Galloway *et al.*, 2021). Therefore, whilst the epitope signals may appear to be similar in the ELISAs presented in this report, carrying out epitope detection chromatography of the cultivars could reveal different subpopulations of this epitope within the HMW exudate that underlie the soil binding differences.

In wheat, xylan polysaccharide epitopes constitute a core element of the putative multi-epitope soil binding complex (Galloway *et al.*, 2020). Two antibodies in particular gave strong signals, LM11 and LM27, and these were chosen to explore heteroxylans in the barley root exudate. One of which, LM11, binds to a 1,4-ß-xylan epitope (McCartney *et al.*, 2005) which was observed presented on root hairs and coating soil particles close to wheat roots (Galloway *et al.*, 2020). To date no clearer evidence has been given of an individual polysaccharide epitope's significance in rhizosheath formation. The LM11 epitope signals in the HMW exudate of Starlight were notably higher than for the other genotypes (Fig.3). This could be linked the greater release of a multi-polysaccharide complex by Starlight, similar to that in wheat. Xylan preparations certainly seem to be important factors of soil binding exudate, a birchwood derived heteroxylan was, at high concentrations, an effective soil binder (Akhtar *et al.*, 2018). But whether the higher signals for the LM11 epitope are directly related to Starlight's soil binding properties is yet to be fully determined and further investigation would be of benefit. The comparative strength of the LM11 epitope in Starlight wasn't maintained in the seedling exudate (Fig.7). Although, Starlight was subject to a considerably smaller sample size and this coupled with the variation of signals observed for a given epitope between

seedlings makes it tricky to determine if this is significant. Conversely the grass xylan epitope LM27 was not seen in the glycan profiling of either forms of Starlight exudate but was detection of the epitope broadly homogenous between the other cultivars. Indeed, Starlight stood out again when comparing the seedling prints with LM27, the overall prints was noticeably weaker than those from the other cultivars. Beatrix and Eunova seedling prints using the LM27 antibody were characterised by sharp serrated outlines to the root prints. This shape and its location suggest root hairs are a factor in these patterns. These differences in heteroxylan epitope profiles between the genotypes indicate the possibility of a genetic basis behind these epitopes within root exudates. Whilst more work investigating this idea is necessary, not least the identification of potential genetic factors governing the synthesis and release of these epitopes, it nevertheless provides the exciting possibility of gene editing or selective breeding programmes to manipulate polysaccharide exudates in root systems . In future studies, immunolabelling of root segments and microscopy of both the detected xylan epitopes is essential. It would provide clarity on the nature of LM27 epitope-root hair associations and also shed light on potential LM11 epitope differences between the cultivars. Whilst the polysaccharide composition of exudates may relate to soil adhesion, the relative amounts of other factors (such as lipids and peptides) compared to the polysaccharide content may also be important (Bacic *et al.*, 1986; Moody *et al.*, 1988; Read *et al.*, 2003). One way to test for this would be to measure the total carbohydrate content of the root exudate by a phenol sulphuric acid-based assay (Masuko *et al.*, 2005). This would provide information on the carbohydrate percentage of the exudate that may help explain differences the soil binding abilities of between the cultivars.

4.2 Polysaccharide exudates as a feature of developmental growth

Both the nitrocellulose seedling printing and the exudate collected from seedlings in water for four hours identified the substantial release of numerous polysaccharide epitopes from young, developing plants. Epitope signals of a single barley seedling left to exude in water for four hours were of comparatively higher strength to processed root exudate of six plants grown in solution for two weeks (Fig. 3 and Fig. 7). The large release of polysaccharides from along the length seedlings could reflect the need for a young plant to rapidly install itself in soil and to curate its microenvironment. The potential developmental significance of root exudate release has been identified previously in other studies, the amount of mucilage released

from seedlings is large (Chaboud, 1983; Read & Gregory, 1997) and younger plants released a greater amount of carbon than mature ones (Gransee & Wittenmayer, 2000; Kuzyakov & Domanski, 2000). A xylogalacturonan epitope (LM8) was ubiquitous in the exudates of seedlings and its release was detected from along the length of the root of in all the cultivars (Fig.7 and Figs.9-12). But it was not found on the root surfaces (Fig.14), or in the HMW exudate of mature plants- consistent with research in wheat (Galloway *et al.*, 2020). The same HMW component of root exudate was used in the soil binding assay, therefore the ability to bind soil in these plants is not associated with this xylogalacturonan epitope. The epitope's prevalent release from the seedlings axes is then likely due to its plant defence and lubricative abilities, but not solely at the root tip as is often reported (Read & Gregory, 1997; Iijima *et al.*, 2004; Durand *et al.*, 2009; Driouich *et al.*, 2013; 2021). An interesting feature was that the LM8 epitope was not found on the tips of the hydroponically grown plant roots a site at where it has traditionally been associated with detaching root cap cells (Fig.15) (Willats *et al.*, 2004). The lack of detection in HMW exudate has been suggested as a consequence of the hydroponics system, with no substrate to provide resistance against the root cap cells at the apex they do not detach (Galloway, 2017). Bringing these ideas together suggests that the LM8 epitope is on a diffuse molecule, that it is shed by the plants through interaction with solid substrate; and that function of this polysaccharide root exudate is vital to a new plant seeking to establish its root system trying to capture resources during an important developmental growth stage.

The different exudate collection processes in this study between seedlings and older plants mean that differences in the epitopes detected may be caused by other factors. As in the case for the LM8 epitope but also for the reduction in strength of the 7E1:B11 epitope in the HMW exudate compared to that collected from seedlings. The hydroponics growth solution is a complex environment with numerous interaction between the roots and the liquid growth medium and it is almost certain the system does not stay completely sterile throughout this time. Any HMW exudate released at the beginning of the two-week growth period is also still in solution at the end. Polysaccharide epitopes in the exudate therefore have a long period of time to be degraded by glycosidases from within the plant cell-wall matrix itself (Franková & Fry, 2013) and fungal or bacterial cell-wall related polysaccharide degrading enzymes (Jones *et al.*, 1972; Cooper & Wood, 1973; Jensen *et al.*, 2008) from possible contamination of the system. Whilst it is likely that glycosidases from

plant cell walls would also affect the exudate of seedlings the comparatively short incubation reduces the time they have to be released. The effect of such enzymes on the hydroponically collected exudate would mean there were fewer epitopes present when surveying by ELISA.

4.3 Function of a novel polysaccharide and glycoprotein elements

Monoclonal antibodies provide coverage of a range of epitopes spanning all manner of polysaccharides and glycoproteins groups. But the detection, with the exception of 7E1:B11, is directed to cell wall polysaccharide epitopes. Whilst exudate undoubtedly contains cell wall polysaccharides from lysed cell contents and detached cells (Read & Gregory, 1997; Cannesan *et al.*, 2012) the likelihood is that root exudate also contains unique plant polysaccharides. Glycosyl-linkage analysis of cereal root exudates (inc. barley) revealed a vast array of monosaccharide linkages (Galloway *et al.*, 2020; 2021) but also, linkages not previously detected in plants before (Bacic *et al.*, 1986). The potential for exudate specific polysaccharides is just beginning to be uncovered with the advent of the 7E1:B11 antibody, which was raised against wheat root exudate and binds to an unknown 1,3-ß-glucan epitope (data unpublished). Whilst other glucan epitopes (JIM6 and 10H2) were detected, the signals were not as strong nor were they seen across all the cultivars as was 7E1:B11. In the investigation, for the first time, this epitope was shown to be abundantly presented on root hairs (Fig.14). Another 1,3-glucan, the fungal derived polysaccharide Pachyman is a highly successful soil binder (Akhtar *et al.*, 2018). These properties make plant 1,3-glucans an important set of molecules for further examination, with regard to rhizosheaths.

The most widely detected class of polysaccharides in the ELISAs of root exudate were glycoproteins, with four related epitopes (AGP; LM2, LM30, LM6-M and extensin; LM1). Arabinogalactan-proteins represent a large class of glycoproteins with a multitude of functions including cell elongation, root hair growth, and root-microbe interactions (Van Hengel & Roberts, 2002; Gaspar *et al.*, 2004; Kirchner *et al.*, 2018). Immunofluorescence microscopy identified the important association of root hairs with the AGP linked LM2 and LM6-M epitopes (Fig.14). In the same way that root hairs increase the surface area for nutrient uptake (Grierson *et al.*, 2014), they also create greater exposure for exudate molecules to the soil interface. It could be that the epitopes detected in conjunction with root hairs are secreted from root hairs or released from elsewhere and then presented on their surface. The

strength of LM6-M signals and its widespread observance; it was the only epitope detected in all the cultivars across all the exudate collection methods, make further exploration into its role essential. Its occurrence in barley root exudate is interesting considering it was not detected in other cereals, in contrast to the LM2 epitope which was found in both wheat and maize exudates (Galloway *et al.*, 2020). A possible explanation to the LM6-M epitope's abundance could be that it is recognising arabinan residues on various AGP populations. Similarly, the AGP epitopes may be shared by a common molecule. A key experiment to discriminate if this was the case, or whether the epitopes represent distinct AGPs, would be separation by sodium dodecyl sulphate (SDS) PAGE (Smallwood *et al.*, 1996). The AGP epitopes were found to have an extensive relationship with root hairs (Fig.14). Indeed, the LM2 epitope appears to be involved in trichoblasts development and root hair formation (Marzec et al., 2015). Root hairs are also a key determinant of rhizosheaths however, the AGP rich gum Arabic, when tested, was a poor soil adhesive (Akhtar *et al.*, 2018). Instead, a capacity of AGPs may be to arrange other adhesive polysaccharides in exudate macromolecules by behaving as cross-linkers between different domains (Cannesan *et al.*, 2012; Tan *et al.*, 2013; Cornuault *et al.*, 2015; Galloway *et al.*, 2020). Due to the diversity of their potential structures, and their functions elsewhere in plant cells (Seifert & Roberts, 2007) it is likely glycoproteins provide other functions in root exudate. Both the LM2 and LM1 extensin epitopes have been identified in defence agents against soil borne root pathogens (Koroney *et al.*, 2016). Sandwich ELISA analysis would provide a good approach to try and identify any links AGPs may form with other polysaccharide molecules and thus the roles they are performing in the barley exudate. Sandwich use provided strong evidence for a soil-binding macromolecule in cereal exudate, which contains multiple different polysaccharide epitopes including AGPs (Galloway *et al.*, 2020). A key aspect of the complex's adhesive action is its corresponding presentation with root hairs, amounts were reduced in the root hairless mutant *brb* compared to its wild type (cv. Pallas) counterpart (Galloway *et al.*, 2021). The identification in this study of AGP epitopes at root hair surfaces implicates them as members of this putative complex. An avenue for subsequent investigations should be using this sandwich ELISAs to probe the Starlight exudate to look for associations between these AGP epitopes presented on root hairs and xylan and xyloglucan substructures to try and gauge an understanding of the composition of any potential soil binding molecules. As well as using the range of cultivar's exudate to discover any anticipated affiliations between 7E1:B11 and other polysaccharide elements.

4.4 Limitations

Despite their versatility, screening with monoclonal antibodies (MAbs) does comes with certain caveats. Monoclonal antibodies, by their nature, can only bind to pre-determined antigens and thus the presence of an unknown molecule in the root's exudates would remain undetected. Although, as long as monoclonal antibodies' use in the investigation of the composition and structure of root exudates, is placed in context alongside other forms of analysis they remain a powerful tool. Some epitopes have been known to mask the epitope of another polysaccharide, preventing the access of MAbs and hence the epitope's detection. Both xyloglucan and mannan epitopes are known to be masked by the presence of pectic homogalacturonan (Marcus *et al.*, 2008; 2010). Pre-treatment of the root used in microscopy with pectic lyase would reveal if this masking was taking place on the root surfaces. But there is also the possibility that there are other instances of epitope masking that are currently unknown, and these could not be tested in this way. Each antibody has its own affinity to its antigen, this requires the cautious interpretation of ELISA signals. High signals indicate abundance of the epitope, but this does not necessarily translate into large amounts of the polysaccharide in the solution. But with these trade-offs in consideration monoclonal antibodies effectiveness is still evident. Their ability for *in situ* analysis of polysaccharides is unmatched. The nature of immunochemical techniques also means they are time efficient compared to other chemical analysis (such as glycosyl linkage analysis or gas chromatography). Owing to the ability of MAbs to be used across different techniques (in this report, glycan profiling by ELISA, immunofluorescence microscopy and nitrocellulose seedling printing) meant multiple facets of polysaccharide root exudates could be explored in a relatively short space of time.

Whilst growing plants in hydroponics maximises the ease in collection of root exudates it is not analogous to growth in soil. Hydroponics differentially alters the root architecture compared with other growth substrates (Liu *et al.*, 2017) and deprives them of root interactions with soil microbes including mycorrhizal associations. It does however remove some of the problems of exudate collection from soils. Hydroponics allows the controlled growth of the plants in terms of resource (light, nutrient, oxygen, and water) access. The breakdown of soil organic matter causes the continual release of molecules (Lehmann & Kleber, 2015) which would contaminate the exudate, and hydroponics allows for the isolation of the root

system ensuring that all the polysaccharides present originate from nowhere else. Collection of root exudate *in situ* from plants grown in soil presented a different set of challenges. The method employed relied on of a build-up of exudate from the six plants in the soil, in similar way to the hydroponics system, and then washing the soil to draw the polysaccharides into the lysimeter. This method is dependent however on how far exudates can travel from the plant. Organic compounds are liable to attaching to soil immobilising them (Dontsova & Bigham, 2005; Jagadamma *et al.*, 2014) and thus, potentially preventing some polysaccharides from being drawn into the lysimeter. A single plant system with the lysimeter in closer proximity could be more effective at collecting exudate at a greater concentration. Collection of exudates from plants in soil also opens the possibility to polysaccharides not of root origin being detected, as was seen with a glucan epitope signals in a no plant control (Fig.13). In future work effective use of a control measure would allow epitopes already contained within the soil and not from the plant to be distinguished.

4.5 Future work

A logical and necessary starting point for future work would be conducting a more extensive rhizosheath screen of barley cultivars. Incorporating more genotypes from the panel screened by George *et al.* (2014) with a focus on those with greatest disparity in rhizosheath weight. As well as with a larger sample size of the current cultivars which would further discriminate the differences in rhizosheath weight. Along with an in-depth phenotyping root hair trait of plants of the same age, this would extend the knowledge of any root hair differences between the lines. Which in turn, would provide clarity to the effect of exudation differences.

Experiments in this investigation have focused on the relationship between polysaccharide factors and soil binding. However, it could be that the polysaccharide factors perform other roles within the rhizosheath. Water retention has been suggested as an important function of exudates and polysaccharide rich mucilage (Young, 1995; Ahmed *et al.*, 2014; Kroener *et al.*, 2014). Grasses have been known to thicken their rhizosheaths in a period of drought (Hartnett *et al*., 2013). It could be then be case that exudate's role in rhizosheath maintenance is marginal until periods of desiccation. Many of the polysaccharide epitopes recognised here may also behave as complex facilitators influencing water dynamics or indeed as soil dispersal agents. Establishing methods to assay

polysaccharides performance in other rhizosheath related functions should also guide future research.

An aspect of this project was to build on the work of polysaccharide exudates in hydroponics and explore *in situ* soil exudate release. Preliminary exploration with the soil suction lysimeter showed that, some of those polysaccharides released by plants in hydroponics could be detected in the soil, and that refinement of the system could potentially identify more. Development of a more robust collection method of exudates from the soil would be beneficial to provide in depth analysis the exudate profiles of barley genotypes. Particularly if, as has been suggested, a solid substrate provides cell deposition that hydroponics does not detect (Galloway, 2017). Soils are complicated environments in which many organisms engage with each other. Exploration of how different soil microbial communities engage with root exudates needs to be understood. The effects of microorganisms own exudates are also likely to impact on those secreted by the root, determining how they both interact to promote particle aggregation and soil stabilization should also be taken into account in future studies.

The genetic factors which provide the basis for the synthesis of polysaccharides destined for release would be a good, if broad, area to explore. The results in this report highlight the anticipated significance of AGPs in exudate. One avenue of exploration could be identifying the protein moiety of the AGP epitope(s) presented on root hairs. An AGP in wheat endosperm, detected by the LM30 epitope shared homology of peptide sequence with of a seed protein (*GSP-1*) (Wilkinson *et al.*, 2017). This provided information on the post translational journey and genetic region of origin of the protein component of the AGP. A high throughput way to screen the potential genes significant to exudate composition could be use of the centrifuge assay developed by Eldridge *et al*. (2021). This has already been used to screen root hair and vesicle trafficking mutant lines. Whilst the method relies on the use of *Arabidopsis* as a model, the large available panel of DNA insertion mutants in *Arabidopsis* make it an appetising way to assess a broad range of potential exudate factors. Mutants used in the screen could include AGP mutants (Schultz *et al.*, 2002) or cell wall polysaccharide mutants deficient in xylan (Brown *et al.*, 2011) and xyloglucan (Cavalier *et al.*, 2008; Park & Cosgrove, 2012)

4.6 Conclusion

The diversity of polysaccharide epitopes detected, as well as differences in those epitopes found at the surface and in the collected exudate, make it unlikely they all share the same function to the plant. The different functions of exudate and the polysaccharides factors that underlie them are only beginning to be understood. The results provided in this report have begun to identify the distinct epitopes associated with soil binding and those epitopes which may provide other services to the root system. A xylogalacturonan (LM8) epitope is on a soluble molecule that can readily move away from the roots surface to modify its surroundings and that this process is especially important for young plants. But the LM6-M, LM2 and 7E1:B11 epitopes represent glycan substructures on a larger complex that is associated with root hair surfaces. The interaction between these root hair surface epitopes and heteroxylan and xyloglucan epitopes could facilitate the adhesion of soil to for rhizosheath formation or represent different functions to the plant entirely. Regardless, glycan rich exudates represent a dynamic mechanism by which roots hold and mould surrounding soil and present an exciting development for future studies.

List of References

Ahmed MA, Kroener E, Benard P, Zarebanadkouki M, Kaestner A, Carminati A. **2016**. Drying of mucilage causes water repellency in the rhizosphere of maize: measurements and modelling. *Plant and Soil* **407**: 161–171.

Ahmed MA, Kroener E, Holz M, Zarebanadkouki M, Carminati A. **2014**. Mucilage exudation facilitates root water uptake in dry soils. *Functional Plant Biology* **41**: 1129–1137.

Akhtar J, Galloway AF, Nikolopoulos G, Field KJ, Knox JP. **2018**. A quantitative method for the high throughput screening for the soil adhesion properties of plant and microbial polysaccharides and exudates. *Plant and Soil* **428**: 57–65.

Asch F, Dingkuhn M, Sow A, Audebert A. **2005**. Drought-induced changes in rooting patterns and assimilate partitioning between root and shoot in upland rice. *Field Crops Research* **93**: 223–236.

Bacic A, Moody SF, Clarke AE. **1986**. Structural Analysis of Secreted Root Slime from Maize (Zea mays L.) . *Plant Physiology* **80**: 771–777.

Barber SA, Walker JM, Vasey EH. **1963**. Mechanisms for the Movement of Plant Nutrients from the Soil and Fertilizer to the Plant Root. *Journal of Agricultural and Food Chemistry* **11**: 204–207.

Bates TR, Lynch JP. **2001**. Root hairs confer a competitive advantage under low phosphorus availability. *Plant and Soil* **236**: 243–250.

Bergmann D, Zehfus M, Zierer L, Smith B, Gabel M. **2009**. Grass rhizosheaths: Associated Bacterial communities and potential for Nitrogen fixation. *Western North American Naturalist* **69**: 105–114.

Brown LK, George TS, Neugebauer K, White PJ. **2017**. The rhizosheath – a potential trait for future agricultural sustainability occurs in orders throughout the angiosperms. *Plant and Soil* **418**: 115–128.

Brown LK, George TS, Thompson JA, Wright G, Lyon J, Dupuy L, Hubbard SF, White PJ. **2012**. What are the implications of variation in root hair length on tolerance to phosphorus deficiency in combination with water stress in barley (Hordeum vulgare)? *Annals of botany* **110**: 319–328.

Brown D, Wightman R, Zhang Z, Gomez LD, Atanassov I, Bukowski JP, Tryfona T, McQueen-Mason SJ, Dupree P, Turner S. **2011**. Arabidopsis genes IRREGULAR XYLEM (IRX15) and IRX15L encode DUF579-containing proteins that are essential for normal xylan deposition in the secondary cell wall. *Plant Journal* **66**: 401–413.

Burak E, Quinton JN, Dodd IC. **2021**. Root hairs are the most important root trait for rhizosheath formation of barley (Hordeum vulgare), maize (Zea mays) and Lotus japonicus (Gifu). *Annals of Botany* **128**: 45–57.

Buwalda G. **1993**. The carbon costs of root systems of perennial fruit crops. *Environmental and Experimental Botany* **33**: 131–140.

Cannesan MA, Durand C, Burel C, Gangneux C, Lerouge P, Ishii T, Laval K, Follet-Gueye ML, Driouich A, Vicré-Gibouin M. **2012**. Effect of arabinogalactan proteins from the root caps of pea and Brassica napus on Aphanomyces euteiches zoospore chemotaxis and germination. *Plant Physiology* **159**: 1658–1670.

Carminati A, Benard P, Ahmed MA, Zarebanadkouki M. **2017**. Liquid bridges at the root-soil interface. *Plant and Soil* **417**: 1–15.

Carpita NC, Gibeaut DM. **1993**. Structural models of primary cell walls in flowering plants: Consistency of molecular structure with the physical properties of the walls during growth. *Plant Journal* **3**: 1–30.

Cassidy ES, West PC, Gerber JS, Foley JA. **2013**. Redefining agricultural yields: From tonnes to people nourished per hectare. *Environmental Research Letters* **8**.

Cavalier DM, Lerouxel O, Neumetzler L, Yamauchi K, Reinecke A, Freshour G, Zabotina OA, Hahn MG, Burgert I, Pauly M, *et al.* 2008. Disrupting two Arabidopsis thaliana xylosyltransferase genes results in plants deficient in xyloglucan, a major primary cell wall component. *Plant Cell* **20**: 1519–1537.

Chaboud A. **1983**. Isolation, purification and chemical composition of maize root cap slime. *Plant and Soil* **73**: 395–402.

Cheng W, Gershenson A. **2007**. Carbon fluxes in the Rhizosphere. In: Cardon ZG, Whitbeck JL, eds. The Rhizopshere; An Ecological Perspective. Academic Press, 31–56.

Cheshire MV, Hayes, M.H.B. 1990. Composition, Origins, Structures, and Reactivities of Soil Polysaccharides. In: M.F. DB, M.H.B. H, A. H, E.B.A. DS, J.J. T, eds. Soil Colloids and Their Associations in Aggregates. Springer, Boston, MA.

Colmer TD, Flowers TJ, Munns R. **2006**. Use of wild relatives to improve salt tolerance in wheat. *Journal of Experimental Botany* **57**: 1059–1078.

Cook BI, Mankin JS, Anchukaitis KJ. **2018**. Climate Change and Drought: From Past to Future. *Current Climate Change Reports* **4**: 164–179.

Cooper RM, Wood RKS. **1973**. Induction of synthesis of extracellular cell-wall degrading enzymes in vascular wilt fungi. *Nature* **246**: 309–311.

Cornuault V, Buffetto F, Rydahl MG, Marcus SE, Torode TA, Xue J, Crépeau MJ, Faria-Blanc N, Willats WGT, Dupree P, *et al.* 2015. Monoclonal antibodies indicate low-abundance links between heteroxylan and other glycans of plant cell walls. *Planta* **242**: 1321–1334.

Cornuault V, Posé S, Knox JP. **2018**. Disentangling pectic homogalacturonan and rhamnogalacturonan-I polysaccharides: Evidence for sub-populations in fruit parenchyma systems. *Food Chemistry* **246**: 275–285.

Delhaize E, James RA, Ryan PR. **2012**. Aluminium tolerance of root hairs underlies genotypic differences in rhizosheath size of wheat (Triticum aestivum) grown on acid soil. *New Phytologist* **195**: 609–619.

Delhaize E, Rathjen TM, Cavanagh CR. **2015**. The genetics of rhizosheath size in a multiparent mapping population of wheat. *Journal of Experimental Botany* **66**: 4527–4536.

Ding W, Yu Z, Tong Y, Huang W, Chen H, Wu P. **2009**. A transcription factor with a bHLH domain regulates root hair development in rice. *Cell Research* **19**: 1309–1311.

Dontsova KM, Bigham JM. **2005**. Anionic Polysaccharide Sorption by Clay Minerals. *Soil Science Society of America Journal* **69**: 1026–1035.

Driouich A, Follet-Gueye ML, Vicré-Gibouin M, Hawes MC. **2013**. Root border cells and secretions as critical elements in plant host defense. *Current Opinion in Plant Biology* **16**: 489–495.

Driouich A, Gaudry A, Pawlak B, Moore JP. **2021**. Root cap–derived cells and mucilage: a protective network at the root tip. *Protoplasma* **339**.

Duell RW, Peacock GR. **1985**. Rhizosheaths on Mesophytic Grasses. *Crop Science* **25**: 880–883.

Durand C, Vicré-Gibouin M, Follet-Gueye ML, Duponchel L, Moreau M, Lerouge P, Driouich A. **2009**. The organization pattern of root border-like cells of Arabidopsis is dependent on cell wall homogalacturonan. *Plant Physiology* **150**: 1411–1421.

Ehdaie B, Layne AP, Waines JG. **2012**. Root system plasticity to drought influences grain yield in bread wheat. *Euphytica* **186**: 219–232.

Eldridge BM, Larson ER, Weldon L, Smyth KM, Sellin AN, Chenchiah I V., Liverpool TB, Grierson CS. **2021**. A Centrifuge-Based Method for Identifying Novel Genetic Traits That Affect Root-Substrate Adhesion in Arabidopsis thaliana. *Frontiers in Plant Science* **12**.

Food and Agriculture Organization of the United Nations. **2018**. FAOSTAT Statistical Database.

Foreman J, Demidchik V, Bothwell JHF, Mylona P, Miedema H, Angel Torres M, Linstead P, Costa S, Brownlee C, Jones JDG, *et al.* 2003. Reactive oxygen species produced by NADPH oxidase regulate plant cell growth. *Nature* **422**: 442–446.

Franková L, Fry SC. **2013**. Biochemistry and physiological roles of enzymes that 'cut and paste' plant cell-wall polysaccharides. *Journal of Experimental Botany* **64**: 3519–3550.

Gahoonia TS, Nielsen NE. **2004**. Barley genotypes with long root hairs sustain high grain yields in low-P field. *Plant and Soil* **262**: 55–62.

Gahoonia TS, Nielsen NE, Joshi PA, Jahoor A. **2001**. A root hairless barley mutant for elucidating genetic of root hairs and phosphorus uptake. *Plant and Soil* **235**: 211–219.

Galloway AF. **2017**. Analysis of Polysaccharides Released by Plant Roots.

Galloway AF, Akhtar J, Burak E, Marcus SE, Field KJ, Dodd C, Knox P. **2021**. A soil-binding polysaccharide complex released from root hairs functions in 1 rhizosheath formation. *bioRxiv*: 2021.04.15.440065.

Galloway AF, Akhtar J, Marcus SE, Fletcher N, Field KJ, Knox JP. **2020**. Cereal root exudates contain highly structurally complex polysaccharides with soil-binding properties. *Plant Journal* **103**: 1666–1678.

Galloway AF, Pedersen MJ, Merry B, Marcus SE, Blacker J, Benning LG, Field KJ, Knox JP. **2018**. Xyloglucan is released by plants and promotes soil particle aggregation. *New Phytologist* **217**: 1128–1136.

Gaspar YM, Nam J, Schultz CJ, Lee LY, Gilson PR, Gelvin SB, Bacic A. **2004**. Characterization of the arabidopsis lysine-rich arabinogalactan-protein AtAGP17 mutant (rat1) that results in a decreased efficiency of agrobacterium transformation. *Plant Physiology* **135**: 2162–2171.

George TS, Brown LK, Ramsay L, White PJ, Newton AC, Bengough AG, Russell J, Thomas WTB. **2014**. Understanding the genetic control and physiological traits associated with rhizosheath production by barley (Hordeum vulgare). *New Phytologist* **203**: 195–205.

Gransee A, Wittenmayer L. **2000**. Qualitative and quantitative analysis of water-soluble root exudates in relation to plant species and development. *Journal of Plant Nutrition and Soil Science* **163**: 381–385.

Grierson C, Nielsen E, Ketelaarc T, Schiefelbein J. **2014**. Root Hairs. In: The

Arabidopsis Book.

Guo MQ, Hu X, Wang C, Lianzhong A. **2017**. Polysaccharides: Structure and Solubility. In: Solubility of Polysaccharides 2. 137–144.

Haling RE, Brown LK, Bengough AG, Valentine TA, White PJ, Young IM, George TS. **2014**. Root hair length and rhizosheath mass depend on soil porosity, strength and water content in barley genotypes. *Planta* **239**: 643–651.

Haling RE, Brown LK, Bengough AG, Young IM, Hallett PD, White PJ, George TS. **2013**. Root hairs improve root penetration, root-soil contact, and phosphorus acquisition in soils of different strength. *Journal of Experimental Botany* **64**: 3711–3721.

Haling RE, Richardson AE, Culvenor RA, Lambers H, Simpson RJ. **2010a**. Root morphology, root-hair development and rhizosheath formation on perennial grass seedlings is influenced by soil acidity. *Plant and Soil* **335**: 457–468.

Haling RE, Simpson RJ, Delhaize E, Hocking PJ, Richardson AE. **2010b**. Effect of lime on root growth, morphology and the rhizosheath of cereal seedlings growing in an acid soil. *Plant and Soil* **327**: 199–212.

Hartnett DC, Wilson GWT, Ott JP, Setshogo M. **2013**. Variation in root system traits among African semi-arid savanna grasses: Implications for drought tolerance. *Austral Ecology* **38**: 383–392.

Harwood WA. **2019**. An Introduction to Barley: The Crop and the Model. In: Harwood WA, Walker JM, eds. Barley: Methods and Protocols. 7–19.

Van Hengel AJ, Roberts K. **2002**. Fucosylated arabinogalactan-proteins are required for full root cell elongation in arabidopsis. *Plant Journal* **32**: 105–113.

Henry A, Cal AJ, Batoto TC, Torre R. ., Serraj R. **2012**. Root attributes affecting water uptake of rice (Oryza sativa) methylation an. *Journal of Experimental Botany* **63**: 475§1-4763.

Henry A, Doucette W, Norton J, Bugbee B. **2007**. Changes in Crested Wheatgrass Root Exudation Caused by Flood, Drought, and Nutrient Stress. *Journal of Environmental Quality* **36**: 904–912.

Hepler PK, Vidali L, Cheung AY. **2001**. Polarised Cell Growth in Higher Plants. *Annual Review of Cell and Developmental Biology* **17**: 159–87.

Hervé C, Knox JP, Marcus SE. **2010**. Monoclonal Antibodies, Carbohydrate-Binding Modules, and the Detection of Polysaccharides in Plant Cell Walls. In: Popper Z., ed. The Plant Cell Wall. Humana Press, Totowa, NJ., 103–113.

Hetherington AM, Brownlee C. **2004**. The generation of Ca2+ signals in plants. *Annual Review of Plant Biology* **55**: 401–427.

Hodge A. **2004**. The plastic plant: Root responses to heterogeneous supplies of nutrients. *New Phytologist* **162**: 9–24.

Hütsch BW, Augustin J, Merbach W. **2002**. Plant rhizodeposition - An important source for carbon turnover in soils. *Journal of Plant Nutrition and Soil Science* **165**: 397–407.

Iijima M, Higuchi T, Barlow PW. **2004**. Contribution of root cap mucilage and presence of an intact root cap in maize (Zea mays) to the reduction of soil mechanical impedance. *Annals of Botany* **94**: 473–477.

Jagadamma S, Mayes MA, Zinn YL, Gísladóttir G, Russell AE. **2014**. Sorption of organic carbon compounds to the fine fraction of surface and subsurface soils. *Geoderma* **213**: 79–86.

James RA, Weligama C, Verbyla K, Ryan PR, Rebetzke GJ, Rattey A, Richardson AE, Delhaize E. **2016**. Rhizosheaths on wheat grown in acid soils: phosphorus acquisition efficiency and genetic control. *Journal of experimental botany* **67**: 3709–3718.

Jensen JK, Sørensen SO, Harholt J, Geshi N, Sakuragi Y, Møller I, Zandleven J, Bernal AJ, Jensen NB, Sørensen C, *et al.* 2008. Identification of a xylogalacturonan xylosyltransferase involved in pectin biosynthesis in Arabidopsis. *Plant Cell* **20**: 1289–1302.

Ji K, Wang Y, Sun W, Lou Q, Mei H, Shen S, Chen H. **2012**. Drought-responsive mechanisms in rice genotypes with contrasting drought tolerance during reproductive stage. *Journal of Plant Physiology* **169**: 336–344.

Jones TM, Anderson AJ, Albersheim P. **1972**. Host-pathogen interactions IV. Studies on the polysaccharide-degrading enzymes secreted by Fusarium oxysporum f. sp. lycopersici. *Physiological Plant Pathology* **2**: 153–166.

Jones DL, Hodge A, Kuzyakov Y. **2004**. Plant and mycorrhizal regulation of rhizodeposition. *New Phytologist* **163**: 459–480.

Jones DD, Morre DJ. **1973**. Golgi Apparatus Mediated Polysaccharide Secretion by Outer Root Cap Cells of Zea mays. III. Control by Exogenous Sugars. *Physiologia Plantarum* **29**: 68–75.

Jones L, Seymour GB, Knox JP. **1997**. Localization of pectic galactan in tomato cell walls using a monoclonal antibody specific to (1→4)-β-D-galactan. *Plant Physiology* **113**: 1405–1412.

Kirchner TW, Niehaus M, Rössig KL, Lauterbach T, Herde M, Küster H, Schenk MK. **2018**. Molecular background of pi deficiency-induced root hair growth in brassica carinata – a fasciclin-like arabinogalactan protein is involved. *Frontiers in Plant Science* **9**: 1–17.

Knox JP, Linstead PJ, Peart J, Cooper C, Roberts K. **1991**. Developmentally regualted epitopes of cell surface arabinogalactan protiens and their relation to root tissue pattern formation. *The Plant Journal* **1**: 317–326.

Kong D, Hu HC, Okuma E, Lee Y, Lee HS, Munemasa S, Cho D, Ju C, Pedoeim L, Rodriguez B, *et al.* 2016. L-Met Activates Arabidopsis GLR Ca2+ Channels Upstream of ROS Production and Regulates Stomatal Movement. *Cell Reports* **17**: 2553–2561.

Koroney AS, Plasson C, Pawlak B, Sidikou R, Driouich A, Menu-Bouaouiche L, Vicré-Gibouin M. **2016**. Root exudate of solanum tuberosum is enriched in galactose-containing molecules and impacts the growth of pectobacterium atrosepticum. *Annals of Botany* **118**: 797–808.

Kosová K, Vítámvás P, Prášil IT. **2014**. Wheat and barley dehydrins under cold, drought, and salinity - What can LEA-II proteins tell us about plant stress response? *Frontiers in Plant Science* **5**: 1–6.

Kroener E, Zarebanadkouki M, Kaestner A, Carminati A. **2014**. Nonequilibrium water dynamics in the rhizosphere: How mucilage affects water flow in soils. *Water Resources Research* **50**: 6479–6495.

Kuzyakov Y, Domanski G. **2000**. Carbon input by plants into the soil. Review. *Journal of Plant Nutrition and Soil Science* **163**: 421–431.

Lee KJD, Marcus SE, Knox JP. **2011**. Cell wall biology: Perspectives from cell wall imaging. *Molecular Plant* **4**: 212–219.

Lehmann J, Kleber M. **2015**. The contentious nature of soil organic matter. *Nature* **528**: 60–68.

Li J, Zhu S, Song X, Shen Y, Chen H, Yu J, Yi K, Liu Y, Karplus VJ, Wu P, *et al.* 2006. A rice glutamate receptor-like gene is critical for the division and survival of individual cells in the root apical meristem. *Plant Cell* **18**: 340–349.

Libault M, Brechenmacher L, Cheng J, Xu D, Stacey G. **2010**. Root hair systems biology. *Trends in Plant Science* **15**: 641–650.

Lister DL, Jones H, Oliveira HR, Petrie CA, Liu X, Cockram J, Kneale CJ, Kovaleva O, Jones MK. **2018**. Barley heads east: Genetic analyses reveal routes of spread through diverse Eurasian landscapes. *PLoS ONE* **13**.

Liu Z, Gao K, Shan S, Gu R, Wang Z, Craft EJ, Mi G, Yuan L, Chen F. **2017**. Comparative analysis of root traits and the associated QTLs for maize seedlings grown in paper roll, hydroponics and vermiculite culture system. *Frontiers in Plant Science* **8**: 1–13.

Lynch JP. **2019**. Root phenotypes for improved nutrient capture: an underexploited opportunity for global agriculture. *New Phytologist* **223**: 548–564.

Lynch JP, Ho MD. **2005**. Rhizoeconomics: Carbon costs of phosphorus acquisition. *Plant and Soil* **269**: 45–56.

Marcus SE, Blake AW, Benians TAS, Lee KJD, Poyser C, Donaldson L, Leroux O, Rogowski A, Petersen HL, Boraston A, *et al.* 2010. Restricted access of proteins to mannan polysaccharides in intact plant cell walls. *Plant Journal* **64**: 191–203.

Marcus SE, Verhertbruggen Y, Hervé C, Ordaz-Ortiz JJ, Farkas V, Pedersen HL, Willats WG, Knox JP. **2008**. Pectic homogalacturonan masks abundant sets of xyloglucan epitopes in plant cell walls. *BMC Plant Biology* **8**: 1–12.

Marzec M, Szarejko I, Melzer M. **2015**. Arabinogalactan proteins are involved in root hair development in barley. *Journal of Experimental Botany* **66**: 1245–1257.

Masood T, Gul R, Munsif F, Jalal F, Hussain Z, Noreen N, Khan HH. **2011**. Effect of Different Phosphorus Levels on the Yield and Yield Components of Maize. *Sarhad Journal Agriculture* **27**: 167–170.

Masuko T, Minami A, Iwasaki N, Majima T, Nishimura SI, Lee YC. **2005**. Carbohydrate analysis by a phenol-sulfuric acid method in microplate format. *Analytical Biochemistry* **339**: 69–72.

Mathesius U, Brundrett M, Ferguson B, Gressshoff P, Filleur S, Munns R, Rasmussen A, Ryan MH, Ryan PR, Schmidt S, *et al.* 2015. Root-soil interface. In: Munns R, Schmidt S, Beveridge C, eds. Plants in Action.

McCartney L, Marcus SE, Knox JP. **2005**. Monoclonal antibodies to plant cell wall xylans and arabinoxylans. *Journal of Histochemistry and Cytochemistry* **53**: 543–546.

McCully M. 1995. Water efflux from the surface of field-grown grass roots. Observations by cryo-scanning electron microscopy. *Physiologia Plantarum* **95**: 217:224.

McCully ME. **1999**. Roots in soil: Unearthing the complexities of roots and their rhizospheres. *Annual Review of Plant Biology* **50**: 695–718.

Montgomery DR. **2007**. Soil erosion and agricultural sustainability. *Proceedings of the National Academy of Sciences of the United States of America* **104**: 13268–13272.

Moody SF, Clarke AE, Bacic A. **1988**. Structural analysis of secreted slime from wheat and cowpea roots. *Phytochemistry* **27**: 2857–2861.

Moreno-Espindola IP, Rivera-Becerril F, de Jesús Ferrara-Guerrero M, De

León-González F. **2007**. Role of root-hairs and hyphae in adhesion of sand particles. *Soil Biology and Biochemistry* **39**: 2520–2526.

Moza J, Gujral HS. **2016**. Starch digestibility and bioactivity of high altitude hulless barley. *Food Chemistry* **194**: 561–568.

Naveed M, Brown LK, Raffan AC, George TS, Bengough AG, Roose T, Sinclair I, Koebernick N, Cooper LJ, Hackett CA, *et al.* 2017. Plant exudates may stabilize or weaken soil depending on species, origin and time. *European Journal of Soil Science* **68**: 806–816.

Newman CW, Newman RK. **2006**. A brief history of barley foods. *Cereal Foods World* **51**: 4–7.

Newton AC, Flavell AJ, George TS, Leat P, Mullholland B, Ramsay L, Revoredo-Giha C, Russell J, Steffenson BJ, Swanston JS, *et al.* 2011. Crops that feed the world 4. Barley: a resilient crop? Strengths and weaknesses in the context of food security. *Food Security* **3**: 141–178.

Nguyen C. **2003**. Rhizodeposition of organic C by plants: mechanisms and controls. *Agronomie* **23**: 375–396.

North GB, Nobel PS. **1997**. Drought-induced changes in soil contact and hydraulic conductivity for roots of Opuntia ficus-indica with and without rhizosheaths. *Plant and Soil* **191**: 249–258.

O'Neill MA, York WS. **2018**. The Composition and Structure of Plant Primary Cell Walls. In: Roberts JA, ed. n Annual Plant Reviews online.

Oburger E, Gruber B, Schindlegger Y, Schenkeveld WDC, Hann S, Kraemer SM, Wenzel WW, Puschenreiter M. **2014**. Root exudation of phytosiderophores from soil-grown wheat. *New Phytologist* **203**: 1161–1174.

Oburger E, Jones DL. **2018**. Sampling root exudates – Mission impossible? *Rhizosphere* **6**: 116–133.

Van Oost K, Quine TA, Govers G, De Gryze S, Six J, Harden JW, Ritchie JC, McCarty GW, Heckrath G, Kosmas C, *et al.* 2007. The impact of agricultural soil erosion on the global carbon cycle. *Science* **318**: 626–629.

Othman AA, Amer WM, Fayez M, Hegazi NA. **2004**. Rhizosheath of sinai desert plants is a potential repository for associative diazotrophs. *Microbiological Research* **159**: 285–293.

Pang J, Ryan MH, Siddique KHM, Simpson RJ. **2017**. Unwrapping the rhizosheath. *Plant and Soil* **418**: 129–139.

Park YB, Cosgrove DJ. **2012**. Changes in cell wall biomechanical properties in the xyloglucan-deficient xxt1/xxt2 mutant of Arabidopsis. *Plant Physiology* **158**: 465–475.

Pattathil S, Avci U, Miller JS, Hahn MG. **2012**. Immunological approaches to plant cell wall and biomass characterization: Glycome profiling. *Methods in Molecular Biology* **908**: 61–72.

Pedersen HL, Fangel JU, McCleary B, Ruzanski C, Rydahl MG, Ralet MC, Farkas V, Von Schantz L, Marcus SE, Andersen MCF, *et al.* 2012. Versatile high resolution oligosaccharide microarrays for plant glycobiology and cell wall research. *Journal of Biological Chemistry* **287**: 39429–39438.

Pimentel D, Burgess M. **2013**. Soil erosion threatens food production. *Agriculture (Switzerland)* **3**: 443–463.

Praba ML, Cairns JE, Babu RC, Lafitte HR. **2009**. Identification of physiological traits underlying cultivar differences in drought tolerance in rice and wheat. *Journal*

of Agronomy and Crop Science **195**: 30–46.

R Core Team. **2018**. R: A language and environment for statistical computing. R Foundation for Statistical Computing, Vienna, Austria.

Rabbi SMF, Tighe MK, Flavel RJ, Kaiser BN, Guppy CN, Zhang X, Young IM. **2018**. Plant roots redesign the rhizosphere to alter the three-dimensional physical architecture and water dynamics. *New Phytologist* **219**: 542–550.

Read DB, Bengough AG, Gregory PJ, Crawford JW, Robinson D, Scrimgeour CM, Young IM, Zhang K, Zhang X. **2003**. Plant roots release phospholipid surfactants that modify the physical and chemical properties of soil. *New Phytologist* **157**: 315–326.

Read DB, Gregory PJ. **1997**. Surface tension and viscosity of axenic maize and lupin root mucilages. *New Phytologist* **137**: 623–628.

Saijo Y, Hata S, Kyozuka J, Shimamoto K, Izui K. **2000**. Over-expression of a single Ca2+-dependent protein kinase confers both cold and salt/drought tolerance on rice plants. *Plant Journal* **23**: 319–327.

Samarah NH. **2005**. Effects of drought stress on growth and yield of barley. *Agronomy for Sustainable Development* **25**: 145–149.

Schultz CJ, Rumsewicz MP, Johnson KL, Jones BJ, Gaspar YM, Bacic A. **2002**. Using genomic resources to guide research directions. The arabinogalactan protein gene family as a test case. *Plant Physiology* **129**: 1448–1463.

Seifert GJ, Roberts K. **2007**. The biology of arabinogalactan proteins. *Annual Review of Plant Biology* **58**: 137–161.

Seymour GB, Colquhoun IJ, Dupont MS, Parsley KR, R. Selvendran R. **1990**. Composition and structural features of cell wall polysaccharides from tomato fruits. *Phytochemistry* **29**: 725–731.

Smallwood M, Yates EA, Willats WGT, Martin H, Knox JP. **1996**. Immunochemical comparison of membrane-associated and secreted arabinogalactan-proteins in rice and carrot. *Planta* **198**: 452–459.

Smith RJ, Hopper SD, Shane MW. **2011**. Sand-binding roots in Haemodoraceae: Global survey and morphology in a phylogenetic context. *Plant and Soil* **348**: 453–470.

Tan L, Eberhard S, Pattathil S, Warder C, Glushka J, Yuan C, Hao Z, Zhu X, Avci U, Miller JS, *et al.* 2013. An Arabidopsis cell wall proteoglycan consists of pectin and arabinoxylan covalently linked to an arabinogalactan protein. *Plant Cell* **25**: 270–287.

The International Barley Genome Sequencing Consortium Principal investigators; Mayer KFX, Waugh R, Langridge P, Close TJ, Wise RP, Graner A, Matsumoto T, Sato K, Schulman A, Ariyadasa R, *et al.* 2012. A physical, genetic and functional sequence assembly of the barley genome. *Nature* **491**: 711–716.

Tilman D, Cassman KG, Matson PA, Naylor R, Polasky S. **2002**. Agricultural sustainability and intensive production practices. *Nature* **418**: 671–677.

Tisdall JM, Oades JM. **1982**. Organic matter and water-stable aggregates in soils. *Journal of Soil Science* **33**: 141–163.

Verhertbruggen Y, Marcus SE, Haeger A, Ordaz-Ortiz JJ, Knox JP. **2009**. An extended set of monoclonal antibodies to pectic homogalacturonan. *Carbohydrate Research* **344**: 1858–1862.

Vermeer J, McCully ME. **1982**. The rhizosphere in Zea: new insight into its

structure and development. *Planta* **156**: 45–61.

Volkens G. **1887**. *Die Flora Der Aegyptisch-Arabischen Wuste: Auf Grundlage Anatomisch-Physiologischer Forschungen*.

Walker TS, Bais HP, Grotewold E, Vivanco JM. **2003**. Update on Root Exudation and Rhizosphere Biology Root Exudation and Rhizosphere Biology 1. *Plant Physiology* **132**: 44–51.

Watt M, McCully ME, Canny MJ. **1994**. Formation and stabilization of rhizosheaths of Zea mays L. Effect of soil water content. *Plant Physiology* **106**: 179–186.

Wilkinson MD, Tosi P, Lovegrove A, Corol DI, Ward JL, Palmer R, Powers S, Passmore D, Webster G, Marcus SE, *et al.* 2017. The Gsp-1 genes encode the wheat arabinogalactan peptide. *Journal of Cereal Science* **74**: 155–164.

Willats WGT, Marcus SE, Knox JP. **1998**. Generation of a monoclonal antibody specific to (1-5)-a-L-arabinan. *Carbohydrate Research* **308**: 149–152.

Willats WGT, Mccartney L, Knox JP. **2001**. In-situ analysis of pectic polysaccharides in seed mucilage and at the root surface of Arabidopsis thaliana. *Planta*: 37–44.

Willats WGT, McCartney L, Steele-King CG, Marcus SE, Mort A, Huisman M, Van Alebeek GJ, Schols HA, Voragen AGJ, Le Goff A, *et al.* 2004. A xylogalacturonan epitope is specifically associated with plant cell detachment. *Planta* **218**: 673–681.

Xue J, Bosch M, Knox JP. **2013**. Heterogeneity and glycan masking of cell wall microstructures in the stems of Miscanthus x giganteus, and its parents M. sinensis and M. sacchariflorus. *PLoS ONE* **8**: 8–11.

Yang Z, Culvenor RA, Haling RE, Stefanski A, Ryan MH, Sandral GA, Kidd DR, Lambers H, Simpson RJ. **2017**. Variation in root traits associated with nutrient foraging among temperate pasture legumes and grasses. *Grass and Forage Science* **72**: 93–103.

Yates EA, Valdor JF, Haslam SM, Morris HR, Dell A, Mackie W, Knox JP. **1996**. Characterization of carbohydrate structural features recognized by anti-arabinogalactan-protein monoclonal antibodies. *Glycobiology* **6**: 131–139.

York LM, Carminati A, Mooney SJ, Ritz K, Bennett MJ. **2016**. The holistic rhizosphere: integrating zones, processes, and semantics in the soil influenced by roots. *Journal of experimental botany* **67**: 3629–3643.

Young IM. **1995**. Variation in moisture contents between bulk soil and the rhizosheath of wheat (Triticum aestivum L. cv. Wembley). *New Phytologist* **130**: 135–139.